Design, Synthesis, and Biological Evaluation of Coumarin Derivatives Tethered to an Edrophonium-like Fragment as Highly Potent and Selective Dual Binding Site Acetylcholinesterase...

ARTICLE *in* CHEMMEDCHEM · SEPTEMBER 2010

Impact Factor: 2.97 · DOI: 10.1002/cmdc.201000210 · Source: PubMed

8 AUTHORS, INCLUDING:

Marco Catto
Università degli Studi di Bari Aldo Moro
49 PUBLICATIONS **1,097** CITATIONS
SEE PROFILE

Orazio Nicolotti
Università degli Studi di Bari Aldo Moro
78 PUBLICATIONS **927** CITATIONS
SEE PROFILE

Angelo Carotti
Università degli Studi di Bari Aldo Moro
225 PUBLICATIONS **4,121** CITATIONS
SEE PROFILE

CHEMMEDCHEM

DOI: 10.1002/cmdc.201000210

Design, Synthesis, and Biological Evaluation of Coumarin Derivatives Tethered to an Edrophonium-like Fragment as Highly Potent and Selective Dual Binding Site Acetylcholinesterase Inhibitors

Leonardo Pisani, Marco Catto, Ilenia Giangreco, Francesco Leonetti, Orazio Nicolotti, Angela Stefanachi, Saverio Cellamare, and Angelo Carotti*[a]

A large series of substituted coumarins linked through an appropriate spacer to 3-hydroxy-*N*,*N*-dimethylanilino or 3-hydroxy-*N*,*N*,*N*-trialkylbenzaminium moieties were synthesized and evaluated as acetylcholinesterase (AChE) and butyrylcholinesterase (BChE) inhibitors. The highest AChE inhibitory potency in the 3-hydroxy-*N*,*N*-dimethylanilino series was observed with a 6,7-dimethoxy-3-substituted coumarin derivative, which, along with an outstanding affinity ($IC_{50} = 0.236$ nM) exhibits excellent AChE/BChE selectivity (SI > 300 000). Most of the synthesized 3-hydroxy-*N*,*N*,*N*-trialkylbenzaminium salts display an AChE affinity in the sub-nanomolar to picomolar range along with excellent AChE/BChE selectivities (SI values up to 138 333). The combined use of docking and molecular dynamics simulations permitted us to shed light on the observed structure–affinity and structure–selectivity relationships, to detect two possible alternative binding modes, and to assess the critical role of π–π stacking interactions in the AChE peripheral binding site.

Introduction

Senile dementia is a progressive neurodegenerative disorder (ND) that affects memory, language, attention, emotions, and problem-solving capabilities. Dementia may be caused by a variety of diseases including Alzheimer's disease (AD), stroke, and other NDs. According to the World Health Organization, AD accounts for two thirds of the cases of dementia observed in nearly 6–10% of the population over 65 years of age in North America.[1] Major clinical hallmarks of AD are the extracellular deposits of β-amyloid peptide (Aβ), derived from amyloid precursor protein (APP) upon cleavage by α- and β-secretases, the intracellular formation of neurofibrillary tangles, constituted mainly by hyperphosphorylated, microtubule-associated tau protein, and the loss of basal forebrain cholinergic neurons.[2–4]

Unfortunately, despite great efforts by public and private research institutions, the leading causes of the onset and progression of AD have not yet been discovered. The lack of this pivotal information has therefore precluded the rational development of a disease-modifying therapy, and indeed the pharmacological approaches in current use are only palliative or target the symptoms.[5] They are based on the restoration of acetylcholine (ACh) through inhibition of acetylcholinesterase (AChE) and on the antagonism the of *N*-methyl-D-aspartate receptor (NMDA), a glutamatergic receptor involved in the neuronal neurotoxicity observed in AD. Five drugs have been marketed for AD (Figure 1). Four are AChE inhibitors (AChEIs): tacrine (1993, Cognex®, later withdrawn mainly because of hepatotoxicity), donepezil (1996, Aricept®), rivastigmine (2000, Exelon®), and galantamine (2001, Reminyl®);[5c] the remainder, memantine (2003, Namenda®), is an NMDA antagonist.[6] Many alternative therapeutic approaches are currently being addressed: these include immunotherapy,[7] neuronal cell regeneration,[8] blockade of Aβ formation and amyloid plaque deposition (with inhibitors of α- and β-secretase, and anti-aggregating and β-sheet-breaking agents),[9] induction of Aβ cerebral clearance,[10] and blockade of tau hyperphosphorylation and aggregation (with kinase inhibitors and anti-aggregating agents, respectively).[11] Despite such large-scale investigations, results from recent AD clinical trials with new experimental drugs have been quite discouraging.[5b,12–14] Less disappointing

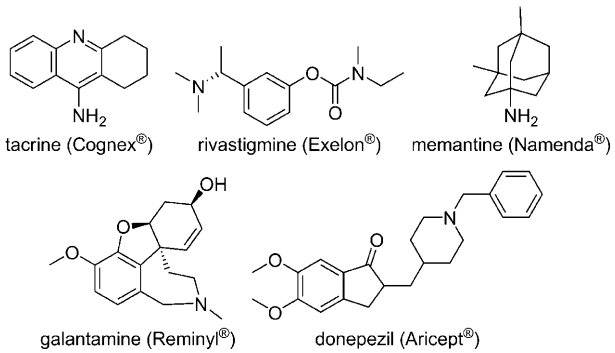

Figure 1. Marketed drugs for the treatment of Alzheimer's disease.

[a] *Dr. L. Pisani, Dr. M. Catto, Dr. I. Giangreco, Dr. F. Leonetti, Dr. O. Nicolotti, Dr. A. Stefanachi, Prof. S. Cellamare, Prof. A. Carotti*
Dipartimento Farmaco-chimico, Università degli Studi di Bari "Aldo Moro"
via Orabona 4, 70125 Bari (Italy)
Fax: (+39) 080-5442230
E-mail: carotti@farmchim.uniba.it

outcomes are expected from preclinical and clinical trials of drugs that address multiple targets of AD.[15,16]

While working on the synthesis and biological evaluation of dual AChE–monoamine oxidase inhibitors,[17,18] we also directed our attention to the design of new AChEIs, with the aim of discovering original and more potent compounds and to clarify the main interactions that occur at the molecular level in the AChE binding sites. AChEIs may act at the primary/catalytic binding sites (e.g., edrophonium and tacrine), at the secondary/peripheral anionic (PAS) binding sites (e.g., propidium and planar heterocyclic uncharged molecules), or at both (e.g., decamethonium and donepezil). In the latter case, efficient interactions at both primary and peripheral binding sites must be ensured by the presence of a linker of appropriate length to tether two identical or different molecular groups for simultaneous binding at the two AChE sites. This simple yet efficient design strategy led to the discovery of potent dual binding site AChEIs, particularly homo-[19] and heterodimers[20a,b] of tacrine and (−)-huperzine A, as well as heterodimers bearing a coumarinic scaffold.[20c] A similar valuable approach deals with the design of multifunctional, chiefly chimeric or hybrid ligands that simultaneously target two or more pathophysiological processes underlying multifactorial illnesses such as NDs.[15a,21] In this emerging and challenging scenario, many multifunctional molecules have been reported in which AChE inhibitor fragments (generally but not exclusively from tacrine, (−)-huperzine A, and close analogues) were conjugated with a molecular moiety profiling the adjunctive targeted activity (e.g., antioxidant,[22] metal chelating,[23] neuroprotective,[17,18,24,25] and anti-amyloidogenic[16c,26]). In the latter case, the design rationale lies in the well-known implication of the PAS of AChE in promoting the aggregation of Aβ into senile plaques.[27] An alternative approach combines the different pharmacological activities into a single non-hybrid molecular structure that is able to modulate different targets, as described by some in our research group[17] and others.[15c,28]

In a recent investigation[29] we reported the synthesis and biological evaluation of a series of amines and quaternary ammonium salts (QASs) bearing an edrophonium-like moiety and a coumarin group as putative ligands at the AChE catalytic and PAS binding sites, respectively, linked by an alkyl chain of appropriate length. The interesting outcomes of that work prompted us to extend the investigation to a new and larger series of derivatives, the fundamental structure of which is illustrated in Figure 2, to explore a greater molecular diversity at the linker and, even more so at the coumarin fragment, with the purpose of deepening our understanding of structure–affinity relationships (SAFIRs) and to discover new molecular entities with therapeutic potential. Notably, all the designed ligands might serve as valuable molecular probes to gain insight into the binding site regions of AChE and, to a lesser extent, butyrylcholinesterase (BChE), the other ChE involved in AD.[30] The designed amine derivatives may be regarded as potential therapeutic agents for AD, whereas the corresponding QASs, due to their inability to cross the blood–brain barrier, may have therapeutic potential in different pathologies such as glaucoma, neuromuscular blockade after surgical anesthesia, and myasthenia gravis.[31] In a highly satisfactory manner, our design led to the discovery of one amine derivative and many QASs endowed with sub-nanomolar affinity toward AChE and outstanding selectivity for AChE over BChE.

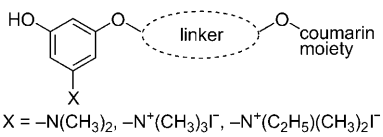

Figure 2. General structure of the synthesized coumarin derivatives.

Results

Chemistry

The synthesis of the 3-hydroxy-*N*,*N*-dimethylanilino derivatives **2**–**20** and their corresponding QASs required the preparation of some common coumarinic building blocks. 6,7-Dimethoxy-3-hydroxycoumarin was prepared from esculetin according to a reported synthetic pathway,[32] with slight modifications; 5- and 8-hydroxycoumarin were synthesized by a Wittig olefination of a suitable hydroxysalicylaldehyde with ethyl (triphenylphosphoranylidene)acetate followed by intramolecular cyclization of the resulting cinnamate ester under very harsh conditions according to a reported procedure,[33] with slight modifications. 7-Hydroxy-3,4-annulated coumarin intermediates **1a** and **1d** were prepared according to the reaction pathway shown in Scheme 1. Classical neat sulfuric acid catalyzed von Pechmann reaction of resorcinol with ethyl 2-oxocyclohexanecarboxylate afforded coumarin **1a**, whose phenolic hydroxy group was protected through methylation to avoid side reactions in the subsequent oxidation reaction carried out by 2,3-dichloro-5,6-dicyano-1,4-benzoquinone (DDQ) in dioxane at reflux. Deprotection with boron tribromide in dichloromethane unmasked the hydroxy group to afford the target coumarin intermediate **1d**.

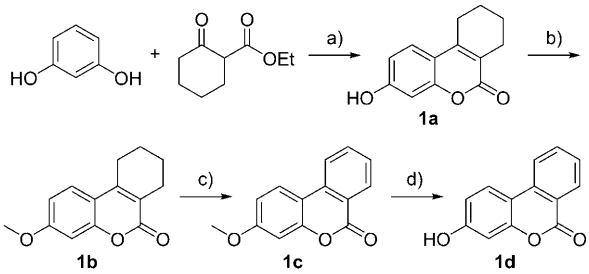

Scheme 1. Reagents and conditions: a) concd H_2SO_4 (cat), 120 °C, 10 min; b) CH_3I, K_2CO_3, DMF (anhyd), RT, 24 h; c) DDQ, dioxane (anhyd), reflux, 24 h; d) BBr_3 (1.0 N in CH_2Cl_2), CH_2Cl_2 (anhyd), RT, 36 h.

Compounds **2**–**7**, **9**, **10**, and **12**–**17**, all bearing a tetramethylene linker, were prepared by a common synthetic pathway illustrated in Scheme 2. The first step was the mono-protection of 5-(dimethylamino)benzene-1,3-diol[34] as a silyl ether with

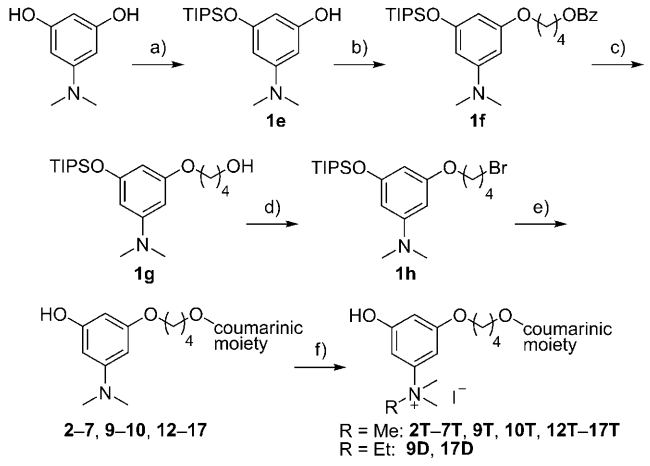

Scheme 2. Reagents and conditions: a) TIPSCl, imidazole, CH_2Cl_2 (anhyd), RT, 2 h; b) $HO(CH_2)_4OBz$, PPh_3, DIAD, THF (anhyd), RT, 15 h; c) LiOH·H_2O, CH_3OH/THF 5:1, RT, 3.5 h; d) CBr_4, PPh_3, CH_2Cl_2 (anhyd), 0 °C→RT, 2 h; e) appropriate hydroxycoumarin, Cs_2CO_3, DMF, H_2O, RT, 24 h then 70 °C, 2 h; f) RI (excess), CH_3CN (anhyd), RT, 24–72 h.

triisopropylsilyl chloride (TIPSCl) in the presence of imidazole as both the base and catalyst. Phenol **1e** served as the nucleophilic component for a standard Mitsunobu coupling with 1,4-butanediol, previously protected as a monobenzoate ester, in the presence of diisopropyl azodicarboxylate (DIAD) and triphenylphosphine. The hydrolysis of **1f** with lithium hydroxide allowed selective removal of the more base-sensitive benzoate protecting group under very mild conditions. Primary alcohol **1g** underwent an Appel bromination with carbon tetrabromide and triphenylphosphine to afford **1h**, which in turn, was treated with the appropriate hydroxycoumarin in *N*,*N*-dimethylformamide in the presence of excess cesium carbonate as the base at room temperature. Subsequent heating at 70 °C enabled a facile cleavage of the silyl protecting group to furnish the targeted 3-hydroxy-*N*,*N*-dimethylanilino derivatives **2**–**7**, **9**, **10**, and **12**–**17**. These derivatives were then transformed into the corresponding *N*,*N*,*N*-trimethyl- and *N*,*N*-dimethyl-*N*-ethylbenzaminium iodides **2T**–**7T**, **9T**, **10T**, **12T**–**17T**, **9D**, and **17D** by reaction with excess methyl or ethyl iodide, respectively, using dry acetonitrile as the solvent.

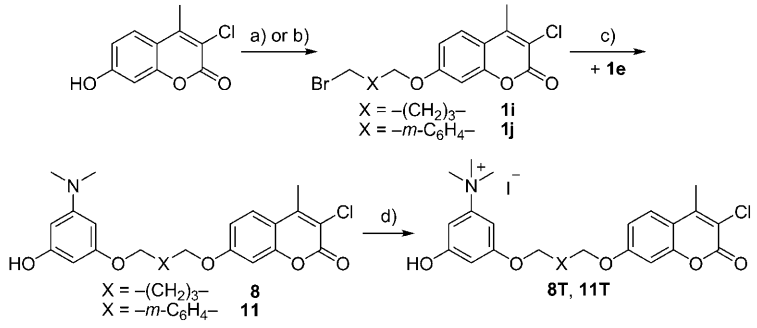

Scheme 3. Reagents and conditions: a) for **1i**: 1,5-dibromopentane, Cs_2CO_3, KI, CH_3CN (anhyd), 160 °C, MW, 1 h; b) for **1j**: 1,3-bis(bromomethyl)benzene, K_2CO_3, THF (anhyd), reflux, 9 h; c) Cs_2CO_3, DMF, H_2O, RT, 24 h then 70 °C, 2 h; d) CH_3I (excess), CH_3CN (anhyd), RT, 24 h.

Schemes 3 and 4 show the synthetic approaches taken to introduce some molecular diversity into the tetramethylene linker, leading to the 3-chloro-4-methyl-7-hydroxy- and 6-hydroxycoumarin derivatives **8**, **11**, and **18**–**20**, respectively. The starting hydroxycoumarins were reacted with *trans*-1,4-dibromo-2-butene or 1,3-bis(bromomethyl)benzene under reflux in tetrahydrofuran and with 1,5-dibromopentane under microwave irradiation in acetonitrile. The reaction of 3-chloro-4-methyl-7-hydroxycoumarin with excess 1,5-dibromopentane or 1,3-bis(bromomethyl)benzene yielded intermediate bromides **1i** and **1j**, respectively, which were then transformed into the final compounds **8** and **11** by a nucleophilic substitution with phenol **1e** (Scheme 3). Amines **8** and **11** were transformed into the corresponding trimethylbenzaminium iodides **8T** and **11T** by reaction with excess methyl iodide in dry acetonitrile at room temperature. In the same manner, 6-hydroxycoumarin was alkylated with excess *trans*-1,4-dibromo-2-butene and 1,5-dibromopentane to afford intermediate bromides **1k** and **1l**, respectively, which, in turn, were reacted with phenol **1e** to give compounds **18** and **19** (Scheme 4). As depicted in Scheme 4, the synthesis of compound **20**, bearing a basic linker, started with the alkylation of 6-hydroxycoumarin with 1,2-dibromoethane in the presence of cesium carbonate and potassium iodide as the catalyst under microwave irradiation. The replacement of bromine in **1m** with 2-methylaminoethanol in THF at reflux afforded **1n**, which was reacted with phenol **1e** under standard Mitsunobu conditions to yield intermediate **1o**. Final desilylation was carried out with tetra-*n*-butylammonium fluoride (TBAF) in THF to afford compound **20**. The *N*,*N*,*N*-trimethylbenzaminium iodides **18T**–**20T** were obtained by treating 3-hydroxy-*N*,*N*-dimethylanilino derivatives **18**–**20** with a large excess of methyl iodide in dry acetonitrile at room temperature.

Biological assays

3-Hydroxy-*N*,*N*-dimethylanilino derivatives **2**–**20** and the corresponding quaternary trialkylammonium salts were tested as inhibitors of bovine AChE and equine serum BChE according to the spectrophotometric method of Ellman et al.[35] The structures and inhibition data toward AChE and BChE, expressed as IC_{50} values or percent inhibition at 10 μM, are listed in Tables 1 and 2. With the exception of the most potent AChE inhibitor **13**, the IC_{50} values of the 3-hydroxy-*N*,*N*-dimethylanilino derivatives were not measured, as their inhibition of BChE was very low (< 50% at 10 μM). Selectivity toward AChE is expressed as the selectivity index SI, that is, the ratio of $(IC_{50\ BChE})/(IC_{50\ AChE})$, whereas the strong affinity increase generally observed in moving from amines to QASs is expressed as the $(IC_{50\ AChE\text{-}amine})/(IC_{50\ AChE\text{-}QAS})$ affinity ratio, AR (Table 2).

Molecular modeling studies

The program GOLD[36] was used in all the docking simulations. In the present investigation, GOLD demonstrated outstanding accuracy in docking donepezil

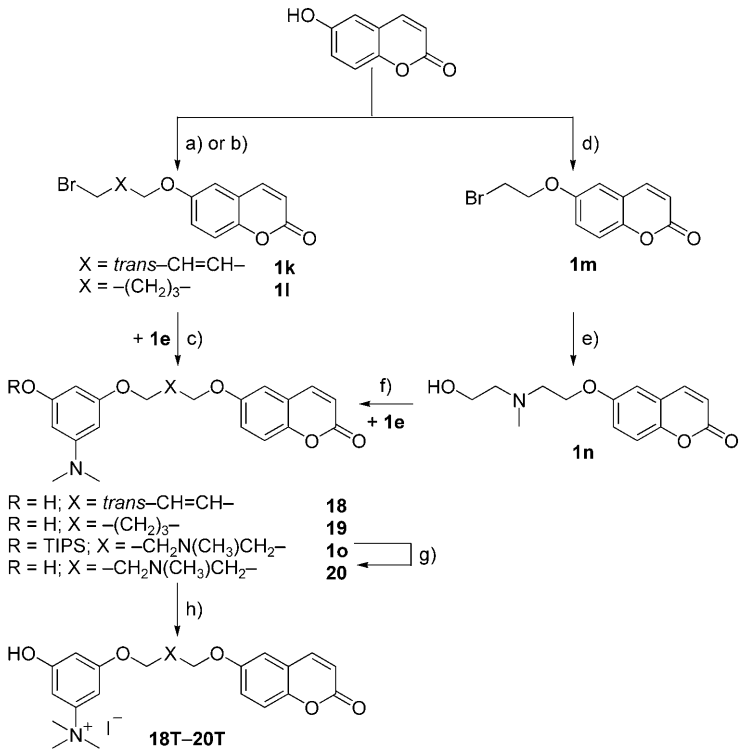

Scheme 4. Reagents and conditions: a) for **1k**: (2*E*)-1,4-dibromo-2-butene, K_2CO_3, THF (anhyd), reflux, 7 h; b) for **1l**: 1,5-dibromopentane, Cs_2CO_3, KI, CH_3CN (anhyd), 160 °C, MW, 1 h; c) for compounds **18** and **19**: Cs_2CO_3, DMF, H_2O, RT, 24 h then 70 °C, 2 h; d) 1,2-dibromoethane, Cs_2CO_3, KI, CH_3CN (anhyd), 160 °C, MW, 1 h; e) 2-methylaminoethanol, DIEA, THF (anhyd), reflux, 15 h; f) for compound **1o**: PPh_3, DIAD, THF (anhyd), 18 h; g) TBAF (1.0 N in THF), THF (anhyd), RT, 30 min; h) CH_3I (excess), CH_3CN (anhyd), RT, 24 h.

into the TcAChE active site, as the deviation from the binding conformation observed in the crystal structure (PDB ID: 1EVE) is very small (RMSD = 0.99 Å). Molecular dynamics (MD) simulations were carried out by using a periodic box of TIP3P water molecules extended for 18 Å from the protein atoms, modeled with the parm03 force field. Energy minimization was executed by using the AMBER 10.0[37] suite, while a 5 ns MD simulation was performed with NAMD.[38]

Discussion

Our molecular design was initially based on the high inhibitory potency toward AChE that was recently observed for compound **6** (IC_{50} = 275 nM, Table 1).[29] This compound was therefore taken as a reference for the evaluation of the SAFIRs.

While maintaining the tetramethylene linker at position 7 of compound **6** unaltered, the substituent effects at positions 3 and 4 of the coumarin ring were explored by synthesizing the unsubstituted, mono-, and disubstituted derivatives **2**–**7**, **9**, and **10**, respectively. Within this series, AChE inhibition data indicate that the substituent lipophilicity plays an important role in inhibitor binding. In fact, the 3-chloro-4-methyl congener **7**, the most lipophilic compound of the series, proved to be fivefold more potent than congener **6** (IC_{50}: 49 versus 275 nM), whereas 3,4-unsubstituted derivative **2** and the two monomethyl-substituted derivatives **3** and **4** were less active than the 3,4-dimethylcoumarin derivative **6**. Moreover, the positive influence of substituent lipophilicity on activity may be appreciated by comparing the affinity of the 4-trifluoromethyl congener **5** (IC_{50} = 60 nM) with the corresponding 4-methyl derivative **4** (IC_{50} = 349 nM). Surprisingly, the highly lipophilic 3,4-cyclohexyl- and 3,4-benzo-fused derivatives **9** and **10**, respectively, were less active than the 3,4-dimethyl congener **6**; this might be ascribed to a likely steric effect exerted by the 3,4-fused rigid ring.

The influence of the length and conformational flexibility of the linker on inhibitory potency was examined with compounds **8**, **11**, **18**, and **19**. Inhibitors **8** and **19**, bearing a pentamethylene linker, are significantly less active than the corresponding inhibitors **7** and **17**, which are characterized by a shorter tetramethylene linker. Moreover, replacement of the central methylene unit of inhibitor **19** with an *N*-methyl group, probably protonated at pH 8 under the conditions of the spectrophotometric biological assay, afforded the less active inhibitor **20**. Unlike other reported findings on homodimeric tacrine derivatives,[39] the insertion of a protonatable nitrogen in the linker, despite undergoing a favorable hydrogen bond interaction with Tyr124, seemed to determine a decrease in affinity for the occurrence of an inverted binding mode. As a matter of fact, molecular docking simulations showed the coumarin and the 3-hydroxy-*N*,*N*-dimethylanilino moieties of **20** bound to the primary and PAS sites, respectively (data not shown). Finally, compounds **11** and **18**, which bear the more rigid *meta*-xylyl and 1,4-butenyl linkers, exhibited lower affinity than the corresponding inhibitors **8** (or **7**) and **17** (or **19**), respectively, which have more flexible polymethylene linkers. The most dramatic decrease in affinity was observed with the *meta*-xylyl linker, from 49 nM (compound **7**), or 161 nM (compound **8**), to 33% inhibition at 10 μM (compound **11**).

Taken together, the above findings coherently suggest that the tetramethylene linker is the ideal spacer in terms of length and conformational flexibility for connecting the 3-hydroxy-*N*,*N*-dimethylanilino and coumarin moieties. Consequently, the tetramethylene linker was kept unaltered in the design of new compounds exploring all the possible anchoring points on the coumarin ring: positions 3 (**12**), 4 (**14**), 5 (**15**), 6 (**17**), and 8 (**16**). The SAFIRs of this new series of inhibitors were evaluated taking the 3,4-unsubstituted 7-alkoxycoumarin derivative **2** as the reference compound.

Derivatives **14**, **15**, and **16**, substituted at the 4-, 5-, and 8-positions, exhibited lower affinity than the corresponding 3-, 6-, and 7-substituted regioisomers **12**, **17**, and **2**, suggesting that lateral substitution at the coumarin ring, i.e., at positions 3, 6, and 7, are preferred over substitutions at positions 4, 5, and 8. The coumarin ring in the 3-, 6-, and 7-substituted derivatives may likely assume a more favorable binding conformation at the PAS pocket of AChE than the corresponding 4-, 5-, and 8-substituted derivatives.

Table 1. Structures and ChE inhibition data for 3-hydroxy-*N*,*N*-dimethylanilino derivatives **2**–**20**.

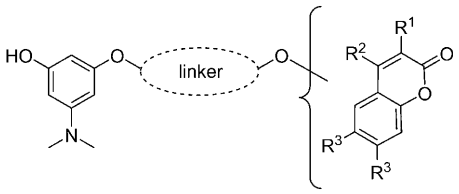

Compd	Linker	C. S.[a]	R^1	R^2	R^3	IC_{50} [nM][b] AChE	BChE
2	$-(CH_2)_4-$	7	H	H	H	456	32%[c]
3	$-(CH_2)_4-$	7	Me	H	H	463	24%[c]
4	$-(CH_2)_4-$	7	H	Me	H	349	38%[c]
5	$-(CH_2)_4-$	7	H	CF_3	H	60.0	23%[c]
6[29]	$-(CH_2)_4-$	7	Me	Me	H	275	25%[c]
7[d]	$-(CH_2)_4-$	7	Cl	Me	H	49.0	2%[c]
8	$-(CH_2)_5-$	7	Cl	Me	H	161	3%[c]
9	$-(CH_2)_4-$	7	$-(CH_2)_4-$		H	333	15%[c]
10	$-(CH_2)_4-$	7	$-(CH{=}CH)_2-$		H	415	12%[c]
11	*m*–$CH_2(C_6H_4)CH_2-$	7	Cl	Me	H	33%[c]	2%[c]
12	$-(CH_2)_4-$	3	–	H	H	143	27%[c]
13[e]	$-(CH_2)_4-$	3	–	H	MeO	0.236	71.0×10^3
14	$-(CH_2)_4-$	4	H	–	H	36.2×10^2	23%[c]
15	$-(CH_2)_4-$	5	H	H	H	13.4×10^2	30%[c]
16	$-(CH_2)_4-$	8	H	H	H	976	45%[c]
17	$-(CH_2)_4-$	6	H	H	H	103	9%[c]
18	*trans*–$CH_2CH{=}CHCH_2-$	6	H	H	H	391	15%[c]
19	$-(CH_2)_5-$	6	H	H	H	164	7%[c]
20	$-(CH_2)_2N(CH_3)(CH_2)_2-$	6	H	H	H	492	49%[c]
donepezil[f]						5.33	2.25×10^3

[a] C.S. = coumarin substitution: linker anchoring positions at the coumarin ring. [b] Data represent the mean value from 2–3 independent experiments (relative SEM < 10%). [c] Percent inhibition at 10 μM (relative SEM < 10%). [d] IC_{50} on human AChE = 194 ± 8.2 nM. [e] IC_{50} on human AChE = 39.7 ± 5.90 nM. [f] IC_{50} on human AChE = 26.0 ± 2.00 nM.

With the aim of further optimizing the AChE binding affinity of compound **12**, two methoxy groups were introduced at positions 6 and 7. A highly satisfactory and dramatic increase in affinity of more than two orders of magnitude was observed with compound **13**, from 143 to 0.236 nM. Although a consistent increase in affinity was eagerly sought, its intensity was rather unexpected when considering previous findings for related AChE inhibitors, such as donepezil.[40]

Kinetics of bovine AChE inhibition by compound **13** revealed a competitive-type inhibition, with $K_i = 2.1 \pm 0.4$ nM. This mechanism differs from that of donepezil and other inhibitors, which supposedly bind at both the catalytic and peripheral sites of AChE. In most cases, mixed or noncompetitive-type inhibitory activity has been reported. Under our experimental conditions, this last mechanism of inhibition was actually demonstrated for donepezil, exhibiting a K_i value of 4.5 ± 0.5 nM. Notably, both **13** and donepezil showed IC_{50} values toward human AChE greater than those toward bovine AChE: 39.7 ± 5.90 and 26.0 ± 2.00 nM, respectively.

The excellent AChE inhibitory potency of compound **13** prompted us to determine its IC_{50} toward BChE as well, to assess its selectivity profile. As expected, a very low BChE affinity was measured (IC_{50} = 71 000 nM), resulting in a SI > 300 000. Compound **13** can therefore be considered a highly active and selective AChE inhibitor with elevated therapeutic potential in AD.

Very low BChE affinities were measured for all the *N*,*N*-dimethylanilino derivatives **2**–**20**, ranging from 2 to 49% enzyme inhibition at a concentration of 10 μM (Table 1). The AChE and BChE inhibition data suggest that these compounds can be regarded as selective, sub-micromolar AChE inhibitors.

3-Hydroxy-*N*,*N*-dimethylanilino derivatives **2**–**20** were transformed into their corresponding *N*,*N*,*N*-trimethylammonium (**T**) and *N*,*N*-dimethyl-*N*-ethylammonium salts (**D**), and their structures and AChE–BChE inhibitory potencies are listed in Table 2. The IC_{50} affinity ratios and selectivity indexes are reported in Table 2 as respective measures of the affinity increase in moving from amines to QASs, and of the enzymatic selectivity.

AChE inhibition data in Table 2 indicate that QASs are much more active than the corresponding amines, exhibiting outstanding sub-nanomolar inhibition potencies, except for compounds **6T**, **11T**, **14T**, and **20T**, the affinities of which remain in the low nanomolar range. The most active AChE inhibitors are compounds **13T** and **17T**, with IC_{50} values of 0.012 and 0.024 nM, respectively. AR values of QASs indicate an affinity increase of approximately three orders of magnitude relative to the corresponding amines, with the notable exception of the bis-QAS **20T**, the low AR of which derives mainly from its relatively low AChE affinity (IC_{50} = 17 nM).

The QASs listed in Table 2 were also evaluated for their affinity toward BChE, and IC_{50} values in the range of 91–2030 nM were measured. The most potent inhibitors are compounds **4T**, **7T**, and **17T**, whereas the least potent compounds are **2T**, **13T**, and **14T**. In contrast to the AChE inhibition data, no defined SAFIR emerged from a comparative analysis of the BChE affinities of the QASs.

The poor BChE inhibitory activity of QASs make them very highly AChE-selective inhibitors, with SI values ranging from 515 (**15T**) to 138 333 (**13T**). Two notable exceptions are compounds **11T** and **20T**, which exhibit SI values as low as 36 and 45, respectively. These rather low figures result mainly from their comparatively weaker AChE inhibitory potency (IC_{50}: 5.8 and 17 nM, respectively) confirming that the *meta*-xylyl and positively charged linkers are unsuitable for favorable interactions at the AChE binding gorge of our inhibitors.

Table 2. Structures and ChE inhibition data for alkylammonium derivatives **2**–**20T**, **9D**, and **17D**.

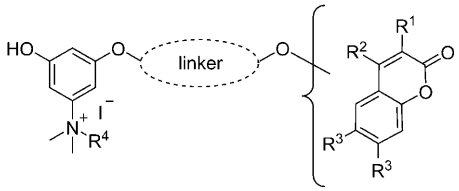

Compd[a]	R^4	IC_{50} [nM][b] AChE	BChE	AR[c]	SI[d]
2T	Me	0.131	14.0×10^2	3481	10687
3T	Me	0.090	499	5144	5544
4T	Me	0.122	91.0	2681	746
5T	Me	0.127	11.6×10^2	472	9134
6T[29]	Me	1.00	708	275	708
7T	Me	0.129	116	380	899
8T	Me	0.114	259	1412	2272
9T	Me	0.208	193	1601	928
9D	Et	0.373	894	893	2397
10T	Me	0.304	11.5×10^2	1365	3783
11T	Me	5.80	206	ND[e]	36
12T	Me	0.0540	200	2648	3704
13T[f]	Me	0.0120	16.6×10^2	20	138333
14T	Me	1.65	20.3×10^2	2194	1230
15T	Me	0.650	335	2062	515
16T	Me	0.310	604	3148	1948
17T	Me	0.0240	137	4292	5708
17D	Et	0.149	680	691	4564
18T	Me	0.217	548	1802	2525
19T	Me	0.151	570	1086	3775
20T[g]	Me	17.0	762	29	45

[a] *N*,*N*-Dimethyl-*N*-ethyl- and *N*,*N*,*N*-trimethylammonium salts of the corresponding coumarins **2**–**20** listed in Table 1 are indicated with capital letters **D** and **T**, respectively; R^1, R^2, and R^3 groups are listed in Table 1. [b] Data represent the mean value from 2–3 independent experiments (relative SEM < 10%). [c] Affinity ratio: $(IC_{50\ AChE\text{-}amine})/(IC_{50\ AChE\text{-}QAS})$. [d] Selectivity index: $(IC_{50\ BChE})/(IC_{50\ AChE})$. [e] Not determinable. [f] IC_{50} on human AChE = 31.0 nM. [g] Compound **20T** is a bis-quaternary ammonium salt bearing a central dimethylammonium group in the linker.

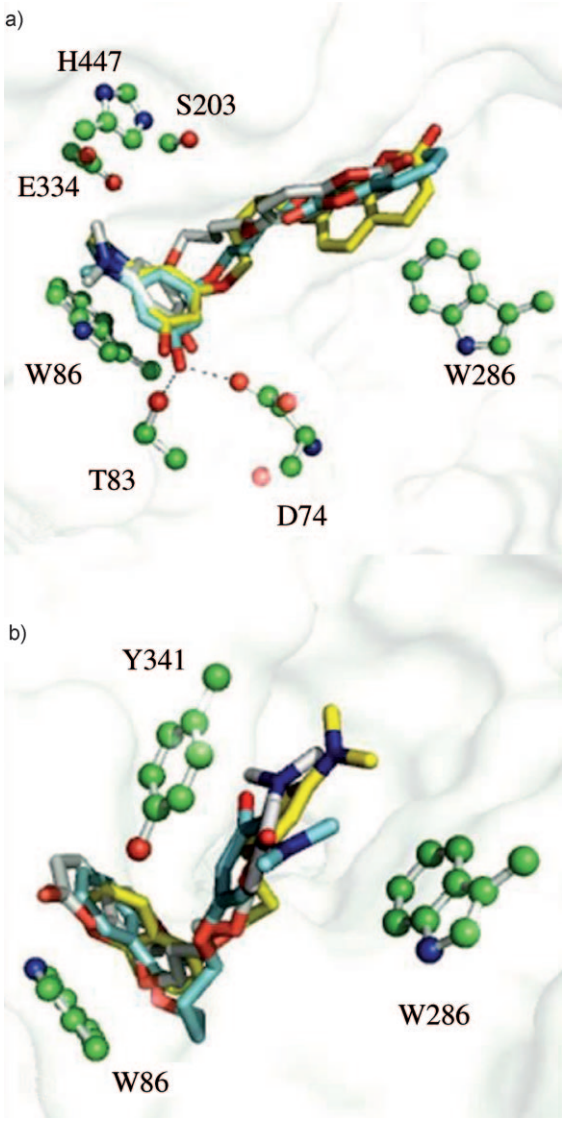

Figure 3. a) Top-scored docking poses of inhibitors **2**, **12**, and **17** (rendered in yellow, cyan, and white capped-stick models, respectively) into the AChE binding sites. Amino acid residues are represented by ball-and-stick models colored according to atom type. Hydrogen bonds are indicated by dark-blue dashed lines. b) Top-scored docking poses of inhibitors **14**, **15**, and **16** (rendered in cyan, yellow, and white capped-stick models, respectively) into the AChE binding sites. Amino acid residues are represented by ball-and-stick models colored according to atom type.

To gain insight into the molecular determinants responsible for high AChE binding affinity and selectivity, anticipated in part in the previous SAFIR analysis, a molecular modeling study was carried out. The objective of this study was threefold: 1) to understand how the remarkable change in AChE affinity is related to the various substituents on the coumarin ring and to the various structural properties of the linker, 2) to rationalize the high AChE affinity of compound **13** resulting from the introduction of two methoxy groups at positions 6 and 7 of 3-substituted coumarin derivative **12**, and 3) to elucidate the excellent enzymatic selectivity observed for compound **13**.

Both docking and molecular dynamics (MD) simulations were performed on wild-type human AChE retrieved from the RCSB Protein Data Bank (hAChE, PDB ID: 1B41),[41] used as a target structure. The GOLD program, used in all docking simulations, was first run on a number of structurally diverse amine inhibitors, i.e., **2**, **12**, and **14**–**17** (Table 1). The binding mode of inhibitors **12**, **17**, and **2**, which carry the linker attached to the coumarin ring at the lateral positions 3, 6, and 7, respectively, and which exhibit higher affinity than the corresponding 4-, 5-, and 8-substituted regioisomers **14**, **15**, and **16**, was initially addressed. The top-scored docking solutions illustrated in Figure 3a indicate that the three inhibitors maintain a similar binding topology irrespective of the anchoring position of the linker to the coumarin ring. More specifically, the 3-hydroxy-*N*,*N*-dimethylanilino moiety is engaged in a π–π stacking interaction with Trp86 located in the AChE catalytic site, and is further stabilized by the formation of two hydrogen bonds between the phenolic hydroxy group and the carboxylate and hydroxy groups of residues Asp74 and Thr83, respectively. The differently bonded coumarin rings are situated in the large hy-

drophobic gorge of the PAS. In comparison with the 3-, 6-, and 7-substituted derivatives **12**, **17**, and **2**, molecular docking simulations of 4-, 5-, and 8-substituted regioisomers **14**, **15**, and **16** resulted in an unexpected inverted binding mode, with the coumarin moiety facing Trp86 at the catalytic binding site and the *N*,*N*-dimethylanilino moiety establishing hydrophobic interactions with the side chain of Tyr341 in the PAS (Figure 3b).

The second step of our investigation was aimed at clarifying the substantial improvement in AChE binding affinity observed in moving from inhibitor **12** to **13**, which differs only in the 6,7-dimethoxy substitution at the coumarin ring. Notably, an increase in affinity, albeit to a much lower extent (nearly 20-fold), had already been observed in going from an unsubstituted 1-indanone moiety to the 5,6-dimethoxy-1-indanone moiety of donepezil.[40] As molecular docking failed to interpret this significant increase in AChE binding affinity for inhibitor **13**, an MD study was undertaken. The top-scored docking poses of **12** and **13** were used as convenient starting geometries for determining the structural variation over time of the two AChE complexes through MD simulations. Both systems were equilibrated according to standard MD protocols.[42] A visual inspection of the molecular frames suggests that the introduction of the two methoxy substituents stabilize the coumarin ring within the PAS in an area largely exposed to the solvent. The two methoxy groups facing the solvent enable inhibitor **13** to insert its coumarin ring into the open slot between the indolic and phenolic rings of Trp286 and Tyr341, respectively. This sandwich-like orientation was maintained throughout the MD simulation and is likely due to a stabilizing π–π stacking interaction (Figure 4). In the primary AChE binding site, inhibitor **13** orients its 3-hydroxy-*N*,*N*-dimethylanilino moiety orthogonally to Trp86 with the *N*,*N*-dimethylamino and phenolic groups establishing a network of hydrogen bonds with two solvent water molecules. Unlike inhibitor **13**, the 6,7-unsubstituted analogue **12** reveals a more pronounced tendency to dive deeper into the AChE gorge to minimize its solvent exposure. Moreover, the stabilizing sandwich-like interaction of coumarin with the Trp286 and Tyr341 side chains was not detected by MD studies, as the coumarin is exclusively engaged in a T-shaped orthogonal π–π interaction with Trp286 or, alternatively, in a parallel π–π interaction with Tyr341 (data not shown).

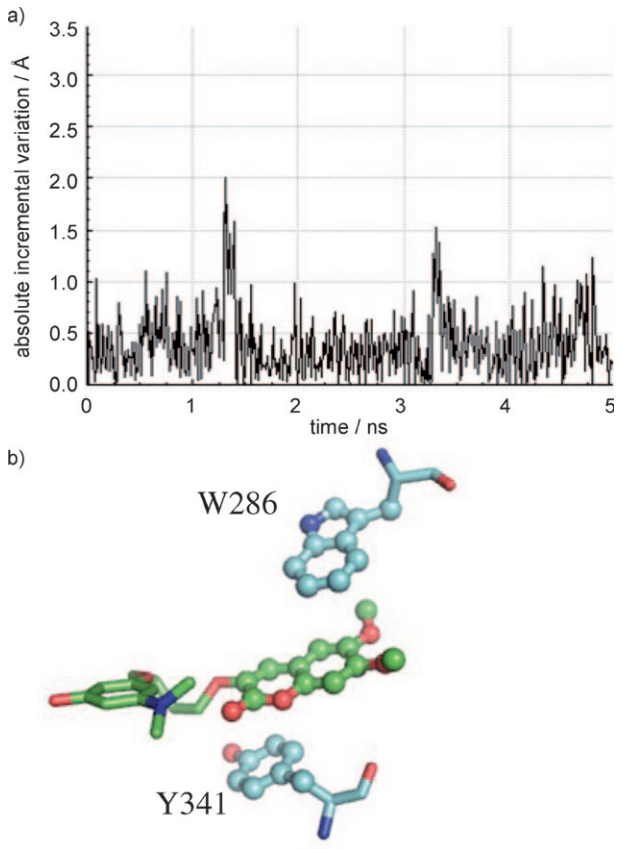

Figure 4. a) Plot showing the absolute incremental variation (from the initial conformations obtained from molecular docking) of the half-sum of distances calculated from the centers of mass of residues W286 and Y341, and the centroid of the coumarin ring of inhibitor **13** over 5 ns MD simulations. b) A representative sandwich-like binding conformation of **13** taken after 5 ns MD simulations.

To interpret the pronounced molecular enzymatic selectivity (SI = 300 847) observed for compound **13**, docking studies on BChE were performed with the human BChE crystal structure (PDB ID: 1POI). The BChE target structure was prepared by following the same procedures described for AChE (see Experimental Section). A comparison between the AChE and BChE top-scored solutions of inhibitor **13** reveal that the 3-hydroxy-*N*,*N*-dimethylanilino moiety is oriented orthogonally to Trp82, as its phenolic and ethereal oxygen atoms interact through hydrogen bonds with Glu197 and Ser198 (BChE numbering) of the catalytic triad, respectively. In addition, the lack of a PAS in BChE does not allow the occurrence of π–π interactions, which are often observed in AChE inhibition (data not shown). The strong AChE/BChE selectivity can therefore be explained mainly by the different molecular binding conformations observed, and is supported, at least in part, by the different energy scores (i.e., 57.27 versus 50.84 kJ mol^{-1}).

Conclusions

Rational structural modifications of 3-hydroxy-*N*,*N*-dimethylanilino derivative **6** led to the discovery of highly potent AChE inhibitors that exhibit binding affinities in the sub-micromolar to sub-nanomolar range (Table 1). SAFIRs clearly indicate that a flexible tetramethylene linker has the optimum length and conformational mobility for high AChE inhibitory potency. Inhibitors equipped with longer or more rigid, or charged/protonated linkers, exhibited a lower potency than the corresponding inhibitors with a tetramethylene linker. Moreover, the anchoring position of the linker to the coumarin ring plays an important role in binding affinity; the 3-, 6-, and 7-substituted derivatives are more potent than the corresponding 4-, 5-, and 8-substituted regioisomers. The highest inhibitory potency in the whole series of 3-hydroxy-*N*,*N*-dimethylanilines was observed with the 6,7-dimethoxy-3-substituted regioisomer **13**, which, along with outstanding potency (IC_{50} = 0.236 nM), exhibits excellent AChE/BChE selectivity (SI = 300 847). This com-

pound can be considered a promising candidate for additional preclinical studies using in vitro and in vivo AD models.

QAS inhibitors (Table 2) showed outstanding AChE inhibitory potencies, from the sub-nanomolar to picomolar range, and an excellent AChE versus BChE selectivity, with SIs generally >1000. Compared with the corresponding 3-hydroxy-*N*,*N*-dimethylanilino derivatives, the AChE inhibitory potency of QASs is nearly three orders of magnitude higher. The most active and selective QAS is the 6,7-dimethoxycoumarin derivative **13T**, with picomolar potency ($IC_{50}=12$ pM) and outstanding selectivity (SI = 138 333). Further studies of **13T** are warranted to assess its pharmacological activity in glaucoma, neuromuscular blockade after surgical anesthesia, and myasthenia gravis. Finally, the combined use of docking and MD simulations has shed light on the SAFIRs observed in our series of amine inhibitors.

Experimental Section

Chemistry

Starting materials, reagents, and analytical-grade solvents were purchased from Sigma–Aldrich (Europe). Microwave (MW) reactions were performed in a Milestone MicroSynth apparatus, setting temperature and hold times, fixing maximum irradiation power to 500 W and ramp times to 5 min. The purity of all intermediates, checked by ^{1}H NMR and HPLC, was always $>95\%$. ^{1}H NMR spectra were recorded in the deuterated solvent specified, at 300 MHz on a Varian Mercury 300 instrument. Chemical shifts (δ) are expressed in parts per million relative to the solvent signal, and the coupling constants (*J*) are given in Hz. The following abbreviations are used: s (singlet), d (doublet), t (triplet), q (quadruplet), h (heptet), dd (double doublet), m (multiplet), br (broad signal); signals due to OH protons were located by deuterium exchange with D_2O. ESIMS analyses were performed on an Agilent 1100 LC–MSD trap system VL. Chromatographic separations were performed on a Biotage SP1 purification system using flash cartridges pre-packed with KP-Sil™ 32–63 μm, 60 Å silica. For reactions requiring the use of anhydrous solvents, glassware was flame-dried and then cooled under a stream of dry argon before use. All reactions were routinely checked by TLC using Merck Kieselgel 60 F_{254} aluminum plates and visualized by UV light or iodine. 7-Hydroxycoumarin, 3-hydroxycoumarin, 7-hydroxy-4-trifluoromethylcoumarin, 6,7-dihydroxycoumarin, 3-chloro-7-hydroxy-4-methylcoumarin, 6-hydroxycoumarin, and 4-hydroxycoumarin were obtained from commercial sources. 7-Hydroxy-4-methylcoumarin,[43] 7-hydroxy-3-methylcoumarin,[44] and 3,4-dimethyl-7-hydroxycoumarin[43] were prepared by following published methods. The purity of all tested final products, determined by reversed-phase (RP) HPLC, was consistently $>98\%$. RP HPLC analyses were performed on a system equipped with automatic injector and a Waters Breeze 1525 pump coupled with a Waters 2489 UV detector using a Waters XTerra RP 5 μm C_8 column (150×3.0 mm i.d.). The UV detection was measured at λ 254 and 280 nm. Each tested compound was analyzed by elution with two different mobile phase systems: in system 1, compounds were eluted with a mixture of CH_3OH/H_2O (80:20 *v*/*v*) at a flow rate of 0.5 mL min^{-1}; in system 2, compounds were eluted with a mixture of CH_3CN/H_2O (65:35 *v*/*v*) at a flow rate of 0.5 mL min^{-1}. The synthesis and spectroscopic data for compound **6** and its corresponding QAS **6T** have been previously reported.[45]

6,7-Dimethoxy-2*H*-chromen-2-one: A Pyrex© vessel was charged with a magnetic stir bar and a Weflon™ heating bar. Esculetin (0.855 g, 4.80 mmol) was added followed by anhydrous acetone (15 mL), CH_3I (2.40 mL, 38.4 mmol), and anhydrous K_2CO_3 (3.32 g, 24.0 mmol). The vessel was placed in a microwave apparatus and irradiated at 110 °C for 30 min. The heating cycle was repeated twice. The mixture was cooled to room temperature, and the inorganic residue was filtered off. The solution was concentrated under reduced pressure to yield the desired product as a yellow solid of satisfactory purity (0.95 g, 96%): ^{1}H NMR (300 MHz, [D_6]DMSO): $\delta=$ 7.94 (d, $J=9.6$ Hz, 1H), 7.26 (s, 1H), 7.05 (s, 1H), 6.28 (d, $J=9.6$ Hz, 1H), 3.84 (s, 3H), 3.78 ppm (s, 3H).

3-Hydroxy-6,7-dimethoxy-2*H*-chromen-2-one: 3-Hydroxy-6,7-dimethoxy-2*H*-chromen-2-one was prepared by following slight modifications of a reported method.[32] 6,7-Dimethoxy-2*H*-chromen-2-one (0.474 g, 2.30 mmol) was dissolved in glacial acetic acid (10 mL). Fuming HNO_3 (0.190 mL) was added, and the mixture was heated at reflux for 30 min. After cooling to room temperature, the mixture was diluted with a mixture of acetic anhydride/acetic acid (1:1 *v*/*v*, 20 mL), and freshly activated zinc powder was added (2.0 g, 30.6 mmol). The reaction mixture was stirred at room temperature for 24 h and then filtered through a Celite™ pad, washing with $CHCl_3$. After evaporation of the solvent, the residue was suspended in H_2O (200 mL) and extracted with $CHCl_3$ (3×80 mL). The organic layers were collected, dried over anhydrous Na_2SO_4, and concentrated to dryness to yield the crude *N*-(6,7-dimethoxy-2-oxo-2*H*-chromen-3-yl)acetamide intermediate, which underwent hydrolysis with 3.0 N aqueous HCl (5 mL) at reflux for 6 h. The mixture was cooled, diluted with cold H_2O (80 mL), and then extracted with EtOAc (3×50 mL). After drying the combined organic layers over anhydrous Na_2SO_4, the removal of the solvent by rotary evaporation yielded a crude solid that was purified by flash chromatography (gradient eluent: EtOAc in *n*-hexane 0→30%) to yield a white solid (0.16 g, 31%): ^{1}H NMR (300 MHz, [D_6]DMSO): $\delta=9.95$ (s, 1H, dis. with D_2O), 7.09 (s, 1H), 7.06 (s, 1H), 7.00 (s, 1H), 3.78 (s, 3H), 3.75 ppm (s, 3H).

3-Hydroxy-7,8,9,10-tetrahydro-6*H*-benzo[*c*]chromen-6-one (1a): Ethyl 2-oxocyclohexanecarboxylate (1.61 mL, 10.0 mmol) and resorcinol (1.10 g, 10.0 mmol) were heated at 120 °C for 10 min with vigorous magnetic stirring after the addition of a few drops of concd H_2SO_4. The solid formed after cooling was washed with EtOAc and filtered to yield **1a** as a white solid (1.54 g, 71%): ^{1}H NMR (300 MHz, [D_6]DMSO): $\delta=10.30$ (s, 1H, dis. with D_2O), 7.51 (d, $J=$ 8.8 Hz, 1H), 6.73–6.77 (m, 1H), 6.66–6.67 (m, 1H), 2.70–2.71 (m, 2H), 2.36–2.38 (m, 2H), 1.67–1.74 ppm (m, 4H).

3-Methoxy-7,8,9,10-tetrahydro-6*H*-benzo[*c*]chromen-6-one (1b): Coumarin derivative **1a** (1.30 g, 6.0 mmol) was dissolved in anhydrous DMF (20 mL). Anhydrous K_2CO_3 (1.25 g, 9.0 mmol) and CH_3I (0.374 mL, 6.0 mmol) were then added. The mixture was stirred at room temperature for 24 h and poured onto crushed ice (200 g). The resulting precipitate was then filtered and washed with H_2O to yield *O*-methylated coumarin derivative **1b** as a white solid (1.35 g, 98%): ^{1}H NMR (300 MHz, [D_6]DMSO): $\delta=7.60$ (d, $J=8.5$ Hz, 1H), 6.93 (s, 1H), 6.89–6.94 (m, 1H), 3.82 (s, 3H), 2.72–2.75 (m, 2H), 2.36–2.39 (m, 2H), 1.66–1.78 ppm (m, 4H).

3-Methoxy-6*H*-benzo[*c*]chromen-6-one (1c): DDQ (2.45 g, 10.8 mmol) was suspended in anhydrous dioxane (30 mL), and then coumarin intermediate **1b** (1.24 g, 3.60 mmol) was added. After holding at reflux for 24 h, the mixture was cooled to room temperature, and the solvent was removed under vacuum. The crude solid residue was dissolved in a mixture of H_2O/EtOAc (3:1

v/v, 600 mL) and extracted with EtOAc (3×150 mL). The organic layers were combined, dried over Na_2SO_4, and concentrated under vacuum. Purification of the resulting solid by flash chromatography (gradient eluent: EtOAc in *n*-hexane 0→10%) yielded coumarin derivative **1c** (0.56 g, 69%): ^{1}H NMR (300 MHz, [D$_6$]DMSO): δ = 8.32 (d, *J* = 8.3 Hz, 1H), 8.26 (d, *J* = 9.1 Hz, 1H), 8.18–8.21 (m, 1H), 7.87–7.92 (m, 1H), 7.56–7.61 (m, 1H), 7.00–7.01 (m, 1H), 6.97–6.98 (m, 1H), 3.85 ppm (s, 3H).

3-Hydroxy-6*H*-benzo[*c*]chromen-6-one (1d): Coumarin derivative **1c** (0.450 g, 1.98 mmol) was dissolved in anhydrous CH_2Cl_2 (15 mL), and a 1.0 N solution of BBr_3 in CH_2Cl_2 (0.590 mL, 5.90 mmol) was added dropwise with simultaneous cooling to 0 °C with an external ice bath. The reaction was slowly warmed to room temperature and then stirred for 36 h. H_2O (50 mL) was added with cooling and stirred for 1 h. The obtained suspension was extracted with CH_2Cl_2 (3×80 mL). The organic layers were collected, dried over anhydrous Na_2SO_4, concentrated under vacuum, and finally purified by flash chromatography (gradient eluent: EtOAc in *n*-hexane 0→20%) to yield the desired *O*-demethylated coumarin intermediate **1d** as a red solid (0.223 g, 53%): ^{1}H NMR (300 MHz, [D$_6$]DMSO): δ = 10.35 (s, 1H, dis. with D_2O), 8.23–8.26 (m, 1H), 8.16–8.18 (m, 1H), 8.14–8.15 (m, 1H), 7.84–7.89 (m, 1H), 7.52–7.57 (m, 1H), 6.81–6.84 (m, 1H), 6.73–6.74 ppm (m, 1H).

2,6-Dihydroxybenzaldehyde: 2,6-Dimethoxybenzaldehyde (0.831 g, 5.0 mmol) was stirred in anhydrous CH_2Cl_2 (50 mL) until complete dissolution. The solution was then cooled to 0 °C, and a 1.0 N solution of BBr_3 in CH_2Cl_2 (20.0 mL, 20.0 mmol) was added dropwise over 30 min. After slow warming to room temperature, the mixture was stirred for 36 h, during which a precipitate formed. The mixture was poured onto crushed ice (500 g) and acidified by the careful addition of a 10% aqueous solution of HCl. The aqueous solution was extracted with EtOAc (3×200 mL), and the organic layers were combined, dried over Na_2SO_4, and concentrated under vacuum. Subsequent purification by flash chromatography (gradient eluent: EtOAc in *n*-hexane 0→20%) gave the desired aldehyde (0.387 g, 56%): ^{1}H NMR (300 MHz, [D$_6$]DMSO): δ = 11.25 (s, 2H, dis. with D_2O), 10.23 (s, 1H), 7.34 (t, *J* = 8.3 Hz, 1H), 6.35 ppm (d, *J* = 8.3 Hz, 2H).

General procedure A for the synthesis of 6- and 8-hydroxycoumarin: The suitable aldehyde (1.0 equiv) was dissolved in *N*,*N*-diethylaniline (20 mL) and ethyl (triphenylphosphoranylidene)acetate (1.5 equiv) was added. The mixture was stirred at room temperature for 2 h and then held at reflux for 1–3 h until TLC monitoring showed disappearance of the starting aldehyde and cinnamate intermediate. The reaction mixture was then cooled and diluted with 6.0 N HCl (150 mL) before extracting with EtOAc (3×100 mL). The organic layers were combined, dried over anhydrous Na_2SO_4, and concentrated under vacuum.

5-Hydroxy-2*H*-chromen-2-one: Prepared according to procedure A, starting from 2,3-dihydroxybenzaldehyde (0.276 g, 2.0 mmol) and ethyl (triphenylphosphoranylidene)acetate (1.05 g, 3.0 mmol). Purification by flash column chromatography (gradient eluent: EtOAc in *n*-hexane 0→20%) yielded the desired aldehyde (0.292 g, 90%): ^{1}H NMR (300 MHz, [D$_6$]DMSO): δ = 10.75 (s, 1H, dis. with D_2O), 8.09 (d, *J* = 9.6 Hz, 1H), 7.38 (t, *J* = 8.3 Hz, 1H), 6.78 (d, *J* = 8.3 Hz, 1H), 6.74 (d, *J* = 8.3 Hz, 1H), 6.31 ppm (d, *J* = 9.6 Hz, 1H).

8-Hydroxy-2*H*-chromen-2-one: Prepared according to procedure A, starting from 2,6-dihydroxybenzaldehyde (0.276 g, 2.0 mmol) and ethyl (triphenylphosphoranylidene)acetate (1.05 g, 3.0 mmol). Purification by flash column chromatography (gradient eluent: EtOAc in *n*-hexane 0→20%) yielded the desired aldehyde (0.159 g, 49%): ^{1}H NMR (300 MHz, [D$_6$]DMSO): δ = 10.17 (s, 1H, dis. with D_2O), 7.99 (d, *J* = 9.6 Hz, 1H), 7.06–7.16 (m, 3H), 6.44 ppm (d, *J* = 9.6 Hz, 1H).

3-(Dimethylamino)-5-[(triisopropylsilyl)oxy]phenol (1e): 5-(Dimethylamino)benzene-1,3-diol[34] (4.60 g, 30.0 mmol) was dissolved in anhydrous CH_2Cl_2 (100 mL), and imidazole (5.11 g, 75.0 mmol) was added to the clear solution. The mixture was cooled to 0–5 °C through an external ice bath, and TIPSCl (6.42 mL, 30.0 mmol) was added dropwise by syringe. The solution was slowly allowed to warm to room temperature and then kept under magnetic stirring for 2 h. H_2O (450 mL) was added, and the aqueous layer was extracted with CH_2Cl_2 (3×200 mL). The organic phases were combined, dried over anhydrous Na_2SO_4, and concentrated under vacuum. The resulting crude yellow oil was purified by flash chromatography (gradient eluent: EtOAc in *n*-hexane 0→20%) to yield a yellow oil that solidified upon standing (8.82 g, 95%): ^{1}H NMR (300 MHz, [D$_6$]DMSO): δ = 8.95 (s, 1H, dis. with D_2O), 5.70–5.71 (m, 1H), 5.63–5.66 (m, 2H), 2.77 (s, 6H), 1.19 (h, *J* = 6.6 Hz, 3H), 1.04 ppm (d, *J* = 6.6 Hz, 18H).

4-Hydroxybutyl benzoate: 1,4-Butanediol (7.44 mL, 84.0 mmol) was suspended in anhydrous CH_3CN (180 mL), and DIPEA (4.70 mL, 27.0 mmol) was added. Benzoyl chloride (3.13 mL, 27.0 mmol), previously dissolved in anhydrous CH_3CN (20 mL), was added dropwise while maintaining the solution at 0–5 °C through an external ice bath. The mixture was stirred for 15 min with cooling and then brought to room temperature and stirred for additional 3 h. The solvent was removed under reduced pressure, and the crude oil was purified by flash chromatography (gradient eluent: EtOAc in *n*-hexane 0→30%) to yield the desired product as a colorless oil (4.82 g, 92%): ^{1}H NMR (300 MHz, $CDCl_3$): δ = 8.02–8.06 (m, 2H), 7.53–7.58 (m, 1H), 7.41–7.47 (m, 2H), 4.36 (t, *J* = 6.3 Hz, 2H), 3.73 (t, *J* = 6.3 Hz, 2H), 1.80–1.92 (m, 2H), 1.68–1.77 (m, 2H), 1.66 ppm (br s, 1H, dis. with D_2O).

4-{3-(Dimethylamino)-5-[(triisopropylsilyl)oxy]phenoxy}butyl benzoate (1f): 4-Hydroxybutyl benzoate (4.27 g, 22.5 mmol) was dissolved in anhydrous THF (63 mL), and then phenol **1e** (8.36 g, 27.0 mmol) was added followed by PPh_3 (7.08 g, 27.0 mmol). The solution was then cooled to 0 °C through an external ice bath, and a solution of DIAD (5.31 mL, 27.0 mmol) in anhydrous THF (27 mL) was added dropwise. The reaction was slowly warmed to room temperature and stirred for 15 h. The solvent was removed under reduced pressure, and the resulting crude mixture was purified by flash chromatography (gradient eluent: EtOAc in *n*-hexane 0→5%), thus obtaining the desired product as a dark-brown oil (10.27 g, 94%): ^{1}H NMR (300 MHz, $CDCl_3$): δ = 8.03–8.06 (m, 2H), 7.53–7.58 (m, 1H), 7.41–7.46 (m, 2H), 5.84–5.91 (m, 3H), 4.39 (t, *J* = 6.1 Hz, 2H), 3.98 (t, *J* = 5.5 Hz, 2H), 2.91 (s, 6H), 1.92–1.98 (m, 4H), 1.21–1.32 (m, 3H), 1.10 ppm (d, *J* = 6.6 Hz, 18H).

4-{3-(Dimethylamino)-5-[(triisopropylsilyl)oxy]phenoxy}butan-1-ol (1g): Benzoate **1f** (7.29 g, 15.0 mmol) was suspended in a mixture of CH_3OH/THF (5:1 *v/v*, 60 mL) and stirred until complete dissolution. LiOH·H_2O (3.15 g, 75.0 mmol) was added, and the reaction was stirred at room temperature for 3.5 h. H_2O (7.5 mL) was added dropwise, and the resulting suspension was kept under stirring for 1 h. The mixture was further diluted with the addition of H_2O (150 mL) and extracted with Et_2O (3×90 mL). The organic layers were collected and washed with a solution of 1.0 N NaOH in H_2O (1×60 mL). The organic phase was dried over Na_2SO_4, and the solvent was removed under vacuum to yield the desired product as a colorless oil (5.15 g, 90%): ^{1}H NMR (300 MHz, $CDCl_3$): δ = 5.86–5.92 (m, 3H), 3.96 (t, *J* = 6.1 Hz, 2H), 3.72 (t, *J* = 5.8 Hz, 2H), 2.91 (s, 6H),

1.82–1.91 (m, 2H), 1.70–1.79 (m, 2H), 1.19–1.31 (m, 3H), 1.11 ppm (d, J=6.9 Hz, 18H), 1 OH not detected.

3-(4-Bromobutoxy)-*N*,*N*-dimethyl-5-[(triisopropylsilyl)oxy]aniline (1h): A solution of alcohol **1g** (4.54 g, 11.9 mmol) in anhydrous CH_2Cl_2 (34 mL) was cooled to 0 °C and CBr_4 (4.34 g, 13.1 mmol) was added. While keeping the reaction mixture at 0 °C, a solution of PPh_3 (3.74 g, 14.3 mmol) in anhydrous CH_2Cl_2 (8.5 mL) was added dropwise. The reaction was slowly allowed to warm to room temperature and stirred for additional 2 h. The resulting crude mixture was then evaporated to dryness and purified by flash chromatography (gradient eluent: EtOAc in *n*-hexane 0→10%) to afford the desired product **1h** (4.34 g, 82%): ^{1}H NMR (300 MHz, $CDCl_3$): δ= 5.83–5.88 (m, 3H), 3.94 (t, J=6.5 Hz, 2H), 3.48 (t, J=6.6 Hz, 2H), 2.90 (s, 6H), 2.01–2.09 (m, 2H), 1.86–1.95 (m, 2H), 1.19–1.31 (m, 3H), 1.11 ppm (d, J=6.9 Hz, 18H).

General procedure B for the preparation of bromides 1i, 1l: A Pyrex© vessel was charged with a magnetic stir bar and a Weflon™ heating bar. The appropriate coumarin (2.0 mmol) was added and dissolved in anhydrous THF (10 mL). Then 1,5-dibromopentane (1.63 mL, 12.0 mmol), Cs_2CO_3 (0.651 g, 2.0 mmol), and KI (0.033 g, 0.2 mmol) were added, and the vessel mixture was placed in the microwave reactor and irradiated at 160 °C for 1 h. After cooling, the mixture was concentrated to dryness.

7-[(5-Bromopentyl)oxy]-3-chloro-4-methyl-2*H*-chromen-2-one (1i): Prepared by following general procedure B, starting from 3-chloro-7-hydroxy-4-methylcoumarin (0.421 g, 2.0 mmol). Purification by flash chromatography (gradient eluent: EtOAc in *n*-hexane 0→20%) afforded **1i** as a white solid (0.626 g, 87%): ^{1}H NMR (300 MHz, $CDCl_3$): δ=7.53 (d, J=8.8 Hz, 1H), 6.89 (dd, J_1=2.5 Hz, J_2=8.8 Hz, 1H), 6.83 (d, J=2.5 Hz, 1H), 4.09 (t, J=6.1 Hz, 2H), 3.41 (t, J=6.1 Hz, 2H), 2.55 (s, 3H), 1.94–2.13 (m, 4H), 1.40–1.45 ppm (m, 2H).

6-[(5-Bromopentyl)oxy]-2*H*-chromen-2-one (1l): Prepared by following general procedure B, starting from 6-hydroxycoumarin (0.324 g, 2.0 mmol). Purification by flash chromatography (gradient eluent: EtOAc in *n*-hexane 0→25%) afforded **1l** as a yellow solid (0.523 g, 84%): ^{1}H NMR (300 MHz, [D$_6$]DMSO): δ=7.98 (d, J= 9.6 Hz, 1H), 7.31 (d, J=9.1 Hz, 1H), 7.27 (d, J=3.0 Hz, 1H), 7.17 (dd, J_1=3.0 Hz, J_2=8.8 Hz, 1H), 6.47 (d, J=9.6 Hz, 1H), 3.99 (t, J= 6.3 Hz, 2H), 3.55 (t, J=6.6 Hz, 2H), 1.85 (q, J=6.6 Hz, 2H), 1.74 (q, J=6.6 Hz, 2H), 1.46–1.59 ppm (m, 2H).

General procedure C for the synthesis of bromides 1j, 1k: A suitable bromide (3.5 mmol) and anhydrous K_2CO_3 (0.278 g, 2.0 mmol) were mixed in anhydrous THF (10 mL) at reflux. The appropriate coumarin (1.0 mmol) was then added portion-wise over 4 h. After completion of the addition, the reaction was heated for an additional 5 h and then cooled to room temperature. The inorganic precipitate was filtered off and washed with THF. The solvent was evaporated under vacuum.

7-{[3-(Bromomethyl)benzyl]oxy}-3-chloro-4-methyl-2*H*-chromen-2-one (1j): Prepared according to procedure C, starting from 1,3-bis(bromomethyl)benzene (0.924 g, 3.5 mmol) and 3-chloro-7-hydroxy-4-methylcoumarin (0.211 g, 1.0 mmol). Purification by flash chromatography (gradient eluent: EtOAc in *n*-hexane 0→30%) afforded **1j** as an off-white solid (0.299 g, 76%): ^{1}H NMR (300 MHz, [D$_6$]DMSO): δ=7.78 (d, J=9.1 Hz, 1H), 7.54 (s, 1H), 7.40–7.41 (m, 3H), 7.13 (d, J=2.5 Hz, 1H), 7.08 (dd, J_1=2.5 Hz, J_2=9.1 Hz, 1H), 5.22 (s, 2H), 4.71 (s, 2H), 2.52 ppm (d, J=9.1 Hz, 3H).

6-{[(2*E*)-4-Bromobut-2-en-1-yl]oxy}-2*H*-chromen-2-one (1k): Prepared according to procedure C, starting from (2*E*)-1,4-dibromo-2-butene (0.749 g, 3.50 mmol) and 6-hydroxycoumarin (0.162 g, 1.0 mmol). Purification by flash chromatography (gradient eluent: EtOAc in *n*-hexane 0→20%) afforded **1k** as a yellow solid (0.186 g, 63%): ^{1}H NMR (300 MHz, [D$_6$]DMSO): δ=7.98 (d, J=9.4 Hz, 1H), 7.33 (d, J=8.8 Hz, 1H), 7.28 (d, J=2.8 Hz, 1H), 7.21 (dd, J_1=2.8 Hz, J_2=8.8 Hz, 1H), 6.48 (d, J=9.4 Hz, 1H), 6.06–6.09 (m, 2H), 4.62–4.63 (m, 2H), 4.12–4.19 (m, 2H).

General procedure D for the synthesis of coumarins 2–7, 9, 10, 12–17: A suitable hydroxycoumarin derivative (0.350 mmol), commercially available or prepared by following the procedures described above, was dissolved in DMF (3.5 mL) followed by the addition of H_2O (70.0 μL) and Cs_2CO_3 (0.326 g, 1.0 mmol). The mixture was stirred for 30 min, then bromide **1h** (0.187 g, 0.420 mmol) was added, and the reaction was stirred for 24 h at room temperature and then heated at 70 °C for 2 h. The solvent was removed by rotary evaporation.

7-{4-[3-(Dimethylamino)-5-hydroxyphenoxy]butoxy}-2*H*-chromen-2-one (2): Prepared by following general procedure D, starting from 7-hydroxycoumarin (0.057 g, 0.35 mmol). Purification by flash chromatography (gradient eluent: EtOAc in *n*-hexane 0→60%) afforded **2** as a white solid (0.084 g, 65%): ^{1}H NMR (300 MHz, [D$_6$]acetone): δ=7.90 (d, J=9.4 Hz, 1H), 7.58 (d, J=8.5 Hz, 1H), 6.94 (dd, J_1=2.5 Hz, J_2=8.5 Hz, 1H), 6.90 (d, J=2.5 Hz, 1H), 6.21 (d, J=9.4 Hz, 1H), 5.85–5.87 (m, 3H), 4.22 (t, J=6.3 Hz, 2H), 4.01 (t, J=6.3 Hz, 2H), 2.86 (s, 6H), 1.92–2.02 ppm (m, 4H), 1 OH not detected; ESIMS *m/z*: 392 $[M+Na]^+$, 368 $[M-H]^-$.

7-{4-[3-(Dimethylamino)-5-hydroxyphenoxy]butoxy}-3-methyl-2*H*-chromen-2-one (3): Prepared by following general procedure D, starting from 7-hydroxy-3-methylcoumarin (0.062 g, 0.35 mmol). Purification by flash chromatography (gradient eluent: EtOAc in *n*-hexane 0→60%) afforded **3** as a white solid (0.105 g, 78%): ^{1}H NMR (300 MHz, [D$_6$]acetone): δ=7.69 (s, 1H), 7.49 (d, J= 8.5 Hz, 1H), 6.88–6.93 (m, 2H), 5.82–5.86 (m, 3H), 4.19 (t, J=6.1 Hz, 2H), 4.01 (t, J=6.1 Hz, 2H), 2.83 (s, 6H), 2.09 (d, J=1.4 Hz, 3H), 1.90–2.01 ppm (m, 4H), 1 OH not detected; ESIMS *m/z*: 406 $[M+Na]^+$, 382 $[M-H]^-$.

7-{4-[3-(Dimethylamino)-5-hydroxyphenoxy]butoxy}-4-methyl-2*H*-chromen-2-one (4): Prepared by following general procedure D, starting from 7-hydroxy-4-methylcoumarin (0.062 g, 0.35 mmol). Purification by flash chromatography (gradient eluent: EtOAc in *n*-hexane 0→60%) afforded **4** as a off-white solid (0.074 g, 55%): ^{1}H NMR (300 MHz, [D$_6$]acetone): δ=7.93 (s, 1H), 7.67 (d, J=8.8 Hz, 1H), 6.95 (dd, J_1=2.5 Hz, J_2=8.8 Hz, 1H), 6.89 (d, J=2.5 Hz, 1H), 6.12 (d, J=1.4 Hz, 1H), 5.80–5.84 (m, 3H), 4.22 (t, J=6.1 Hz, 2H), 4.01 (t, J=6.1 Hz, 2H), 2.83 (s, 6H), 2.44 (d, J= 1.4 Hz, 3H),1.91–2.02 ppm (m, 4H); ESIMS *m/z*: 406 $[M+Na]^+$, 382 $[M-H]^-$.

7-{4-[3-(Dimethylamino)-5-hydroxyphenoxy]butoxy}-4-(trifluoromethyl)-2*H*-chromen-2-one (5): Prepared by following general procedure D, starting from 7-hydroxy-4-trifluoromethylcoumarin (0.081 g, 0.35 mmol). Purification by flash chromatography (gradient eluent: EtOAc in *n*-hexane 0→50%) afforded **5** as a dark-pink solid (0.107 g, 70%): ^{1}H NMR (300 MHz, [D$_6$]DMSO): δ=9.00 (s, 1H, dis. with D_2O), 7.58–7.61 (m, 1H), 7.13–7.14 (m, 1H), 7.03–7.06 (m, 1H), 6.84 (s, 1H), 5.68–5.70 (m, 3H), 4.14–4.18 (m, 2H), 3.89–3.92 (m, 2H), 2.78 (s, 6H), 1.81–1.85 (m, 4H); ESIMS *m/z*: 460 $[M+Na]^+$, 436 $[M-H]^-$.

3-Chloro-7-{4-[3-(dimethylamino)-5-hydroxyphenoxy]butoxy}-4-methyl-2*H*-chromen-2-one (7): Prepared by following general procedure D, starting from 3-chloro-7-hydroxy-4-methylcoumarin

(0.074 g, 0.35 mmol). Purification by flash chromatography (gradient eluent: EtOAc in *n*-hexane 0→30%) afforded **7** as a yellow solid (0.097 g, 66%): ^{1}H NMR (300 MHz, $CDCl_3$): δ=7.51 (d, J=8.8 Hz, 1H), 6.89 (dd, J_1=2.2 Hz, J_2=8.8 Hz, 1H), 6.83 (d, J=2.2 Hz, 1H), 5.84–5.88 (m, 3H), 4.10 (t, J=6.1 Hz, 2H), 4.00 (t, J=5.8 Hz, 2H), 2.90 (s, 6H), 2.55 (s, 3H), 1.94–2.02 ppm (m, 4H), 1 OH not detected; ESIMS *m/z* (%): 440 (100) $[M+Na]^+$, 442 (36), 416 (100) $[M-H]^-$, 418 (35).

3-{4-[3-(Dimethylamino)-5-hydroxyphenoxy]butoxy}-7,8,9,10-tetrahydro-6*H*-benzo[*c*]chromen-6-one (9): Prepared by following general procedure D, starting from **1a** (0.076 g, 0.35 mmol). Purification by flash chromatography (gradient eluent: EtOAc in *n*-hexane 0→40%) afforded **9** as a brown solid (0.086 g, 58%): ^{1}H NMR (300 MHz, $[D_6]$DMSO): δ=8.99 (s, 1H, dis. with. D_2O), 7.60 (d, J=8.5 Hz, 1H), 6.90–6.94 (m, 2H), 5.67–5.70 (m, 3H), 4.10 (t, J=5.8 Hz, 2H), 3.90 (t, J=5.8 Hz, 2H), 2.78 (s, 6H), 2.71–2.75 (m, 2H), 2.38–2.40 (m, 2H), 1.78–1.86 (m, 4H), 1.68–1.75 ppm (m, 4H); ESIMS *m/z*: 446 $[M+Na]^+$, 422 $[M-H]^-$.

3-{4-[3-(Dimethylamino)-5-hydroxyphenoxy]butoxy}-6*H*-benzo[*c*]chromen-6-one (10): Prepared by following general procedure D, starting from **1d** (0.074 g, 0.35 mmol). Purification by flash chromatography (gradient eluent: EtOAc in *n*-hexane 0→30%) afforded **10** as a red solid (0.103 g, 70%): ^{1}H NMR (300 MHz, $[D_6]$acetone): δ=8.26–8.29 (m, 2H), 8.20 (d, J=9.1 Hz, 1H), 7.87–7.93 (m, 1H), 7.57–7.63 (m, 1H), 7.01 (dd, J_1=2.5 Hz, J_2=8.8 Hz, 1H), 6.95 (d, J=2.5 Hz, 1H), 5.82–5.85 (m, 3H), 4.23 (t, J=6.1 Hz, 2H), 4.02 (t, J=6.1 Hz, 2H), 2.86 (s, 6H), 1.91–2.02 ppm (m, 4H), 1 OH not detected; ESIMS *m/z*: 442 $[M+Na]^+$, 418 $[M-H]^-$.

3-{4-[3-(Dimethylamino)-5-hydroxyphenoxy]butoxy}-2*H*-chromen-2-one (12): Prepared by following general procedure D, starting from 3-hydroxycoumarin (0.057 g, 0.35 mmol). Purification by flash chromatography (gradient eluent: EtOAc in *n*-hexane 0→30%) afforded **12** as a white solid (0.081 g, 63%): ^{1}H NMR (300 MHz, $CDCl_3$): δ=7.31–7.40 (m, 3H), 6.84–6.91 (m, 2H), 5.80–5.88 (m, 3H), 4.10 (t, J=5.8 Hz, 2H), 4.01 (t, J=5.8 Hz, 2H), 2.89 (s, 6H), 1.96–2.17 ppm (m, 4H), 1 OH not detected; ESIMS *m/z*: 392 $[M+Na]^+$, 368 $[M-H]^-$.

3-{4-[3-(Dimethylamino)-5-hydroxyphenoxy]butoxy}-6,7-dimethoxy-2*H*-chromen-2-one (13): Prepared by following general procedure D, starting from 3-hydroxy-6,7-dimethoxycoumarin obtained as previously described (0.078 g, 0.35 mmol). Purification by flash chromatography (gradient eluent: EtOAc in *n*-hexane 0→60%) afforded **13** as a white solid (0.096 g, 64%): ^{1}H NMR (300 MHz, $[D_6]$DMSO): δ=9.00 (s, 1H, dis. with D_2O), 7.28 (s, 1H), 7.11 (s, 1H), 7.02 (s, 1H), 5.70 (m, 3H), 4.02 (t, J=5.8 Hz, 2H), 3.92 (t, J=5.8 Hz, 2H), 3.80 (s, 3H), 3.76 (s, 3H), 2.78 (s, 6H), 1.81–1.89 ppm (m, 4H); ESIMS *m/z*: 452 $[M+Na]^+$, 428 $[M-H]^-$.

4-{4-[3-(Dimethylamino)-5-hydroxyphenoxy]butoxy}-2*H*-chromen-2-one (14): Prepared by following general procedure D, starting from 4-hydroxycoumarin (0.057 g, 0.35 mmol). Purification by flash chromatography (gradient eluent: EtOAc in *n*-hexane 0→70%) afforded **14** as a white solid (0.093 g, 72%): ^{1}H NMR (300 MHz, $[D_6]$DMSO): δ=9.00 (s, 1H, dis. with D_2O), 7.77–7.80 (m, 1H), 7.61–7.67 (m, 1H), 7.30–7.40 (m, 2H), 5.89 (s, 1H), 5.69–5.70 (m, 3H), 4.26 (t, J=6.1 Hz, 2H), 3.94 (t, J=6.3 Hz, 2H), 2.78 (s, 6H), 1.84–1.97 ppm (m, 4H); ESIMS *m/z*: 392 $[M+Na]^+$, 368 $[M-H]^-$.

5-{4-[3-(Dimethylamino)-5-hydroxyphenoxy]butoxy}-2*H*-chromen-2-one (15): Prepared by following general procedure D, starting from 5-hydroxycoumarin (0.057 g, 0.35 mmol). Purification by flash chromatography (gradient eluent: EtOAc in *n*-hexane 0→60%) afforded **15** as a off-white solid (0.089 g, 69%): ^{1}H NMR (300 MHz, $[D_6]$DMSO): δ=9.00 (s, 1H, dis. with D_2O), 8.08 (d, J=9.6 Hz, 1H), 7.53 (t, J=8.5 Hz, 1H), 6.92–6.95 (m, 2H), 6.34 (d, J=9.6 Hz, 1H), 5.67–5.70 (m, 3H), 4.17 (t, J=6.1 Hz, 2H), 3.93 (t, J=5.8 Hz, 2H), 2.78 (s, 6H), 1.87–1.91 ppm (m, 4H); ESIMS *m/z*: 392 $[M+Na]^+$, 368 $[M-H]^-$.

8-{4-[3-(Dimethylamino)-5-hydroxyphenoxy]butoxy}-2*H*-chromen-2-one (16): Prepared by following general procedure D, starting from 8-hydroxycoumarin (0.057 g, 0.35 mmol). Purification by flash chromatography (gradient eluent: EtOAc in *n*-hexane 0→50%) afforded **16** as a white solid (0.075 g, 58%): ^{1}H NMR (300 MHz, $[D_6]$DMSO): δ=9.00 (s, 1H, dis. with D_2O), 8.03 (d, J=9.6 Hz, 1H), 7.24–7.32 (m, 3H), 6.48 (d, J=9.6 Hz, 1H), 5.69 (br s, 3H), 4.15 (t, J=6.1 Hz, 2H), 3.92 (t, J=5.8 Hz, 2H), 2.78 (s, 6H), 1.82–1.93 ppm (m, 4H); ESIMS *m/z*: 392 $[M+Na]^+$, 368 $[M-H]^-$.

6-{4-[3-(Dimethylamino)-5-hydroxyphenoxy]butoxy}-2*H*-chromen-2-one (17): Prepared by following general procedure D, starting from 6-hydroxycoumarin (0.057 g, 0.35 mmol). Purification by flash chromatography (gradient eluent: EtOAc in *n*-hexane 0→70%) afforded **14** as a white solid (0.079 g, 61%): ^{1}H NMR (300 MHz, $[D_6]$DMSO): δ=8.99 (s, 1H, dis. with D_2O), 7.97 (d, J=9.6 Hz, 1H), 7.32 (d, J=9.1 Hz, 1H), 7.27 (d, J=2.8 Hz, 1H), 7.18 (dd, J_1=2.8 Hz, J_2=9.1 Hz, 1H), 6.47 (d, J=9.6 Hz, 1H), 5.67–5.70 (m, 3H), 4.05 (t, J=6.1 Hz, 2H), 3.90 (t, J=5.8 Hz, 2H), 2.78 (s, 6H), 1.79–1.87 ppm (m, 4H); ESIMS *m/z*: 392 $[M+Na]^+$, 368 $[M-H]^-$.

General procedure E for the synthesis of coumarin derivatives 8, 11, 18–19: Phenol **1e** (0.108 g, 0.350 mmol), was dissolved in DMF (3.5 mL) followed by the addition of H_2O (70.0 μL) and Cs_2CO_3 (0.326 g, 1.0 mmol). The mixture was stirred for 30 min at room temperature, then a suitable bromide **1i,j** or **1k,l** (0.420 mmol) was added, and the reaction was stirred for additional 24 h and then heated at 70 °C for 2 h. The solvent was removed by rotary evaporation.

3-Chloro-7-({5-[3-(dimethylamino)-5-hydroxyphenoxy]pentyl}oxy)-4-methyl-2*H*-chromen-2-one (8): Prepared by following general procedure E, starting from bromide **1i** (0.151 g, 0.42 mmol). Purification by flash chromatography (gradient eluent: EtOAc in *n*-hexane 0→30%) afforded **8** as a white solid (0.083 g, 55%): ^{1}H NMR (300 MHz, $[D_6]$DMSO): δ=8.98 (s, 1H, dis. with D_2O), 7.74 (d, J=8.8 Hz, 1H), 7.03 (d, J=2.5 Hz, 1H), 6.99 (dd, J_1=2.5 Hz, J_2=8.8 Hz, 1H), 5.67–5.69 (m, 3H), 4.09 (t, J=6.6 Hz, 2H), 3.85 (t, J=6.3 Hz, 2H), 2.78 (s, 6H), 2.52 (s, 3H), 1.67–1.80 (m, 4H),1.50–1.58 ppm (m, 2H); ESIMS *m/z*: 454 (100) $[M+Na]^+$, 456 (34), 430 (100) $[M-H]^-$, 432 (35).

3-Chloro-7-[(3-{[3-(dimethylamino)-5-hydroxyphenoxy]methyl}benzyl)oxy]-4-methyl-2*H*-chromen-2-one (11): Prepared by following general procedure E, starting from bromide **1j** (0.165 g, 0.42 mmol). Purification by flash chromatography (gradient eluent: EtOAc in *n*-hexane 0→40%) afforded **11** as a white solid (0.092 g, 57%): ^{1}H NMR (300 MHz, $[D_6]$acetone): δ=7.96 (s, 1H, dis. with D_2O), 7.77 (d, J=8.8 Hz, 1H), 7.62 (s, 1H), 7.43–7.48 (m, 3H), 7.09 (dd, J_1=2.5 Hz, J_2=8.8 Hz, 1H), 7.04 (d, J=2.5 Hz, 1H), 5.85–5.91 (m, 3H), 5.31 (s, 2H), 5.07 (s, 2H), 2.86 (s, 6H), 2.59 ppm (s, 3H); ESIMS *m/z*: 488 (100) $[M+Na]^+$, 490 (37), 464 (100) $[M-H]^-$, 466 (35).

6-({(2*E*)-4-[3-(Dimethylamino)-5-hydroxyphenoxy]but-2-en-1-yl}oxy)-2*H*-chromen-2-one (18): Prepared by following general procedure E, starting from bromide **1k** (0.124 g, 0.42 mmol). Purification by flash chromatography (gradient eluent: EtOAc in *n*-hexane 0→60%) afforded **18** as a red solid (0.080 g, 62%): ^{1}H NMR

(300 MHz, [D$_6$]DMSO): δ = 9.02 (s, 1H, dis. with D$_2$O), 7.97 (d, J = 9.6 Hz, 1H), 7.33 (d, J = 8.8 Hz, 1H), 7.28 (d, J = 3.0 Hz, 1H), 7.21 (dd, J_1 = 3.0 Hz, J_2 = 8.8 Hz, 1H), 6.47 (d, J = 9.6 Hz, 1H), 6.01–6.04 (m, 2H), 5.71 (m, 3H), 4.62–4.63 (m, 2H), 4.48 (br s, 2H), 2.78 ppm (s, 6H); ESIMS m/z: 390 [M+Na]$^+$, 366 [M−H]$^-$.

6-({5-[3-(Dimethylamino)-5-hydroxyphenoxy]pentyl}oxy)-2*H*-chromen-2-one (19): Prepared by following general procedure E, starting from bromide **1l** (0.131 g, 0.42 mmol). Purification by flash chromatography (gradient eluent: EtOAc in *n*-hexane 0→50%) afforded **19** as a white solid (0.064 g, 48%): ^{1}H NMR (300 MHz, [D$_6$]DMSO): δ: 8.97 (s, 1H, dis. with D$_2$O), 7.97 (d, J = 9.6 Hz, 1H), 7.31 (d, J = 9.1 Hz, 1H), 7.26 (d, J = 2.8 Hz, 1H), 7.18 (dd, J_1 = 2.8 Hz, J_2 = 9.1 Hz, 1H), 6.46 (d, J = 9.6 Hz, 1H), 5.68–5.70 (m, 3H), 4.01 (t, J = 6.3 Hz, 2H), 3.85 (t, J = 6.1 Hz, 2H), 2.78 (s, 6H), 1.67–1.82 (m, 4H), 1.53–1.58 ppm (m, 2H); ESIMS m/z: 406 [M+Na]$^+$, 382 [M−H]$^-$.

6-(2-Bromoethoxy)-2*H*-chromen-2-one (1m): In a Pyrex© vessel charged with a magnetic stir bar and a Weflon™ heating bar, 6-hydroxycoumarin (0.973 g, 6.0 mmol) was dissolved in anhydrous THF (15 mL), and then 1,2-dibromoethane (3.10 mL, 36.0 mmol), Cs_2CO_3 (1.95 g, 6.0 mmol), and KI (0.100 g, 0.60 mmol) were added. The mixture was heated by microwave irradiation to 150 °C for 1 h, then cooled, and the irradiation cycle was repeated. The mixture was cooled, filtered, and the solution was concentrated and purified by flash chromatography (gradient eluent: EtOAc in *n*-hexane 0→25%) to give the desired coumarin derivative **1m** as a white solid (0.727 g, 45%): ^{1}H NMR (300 MHz, $CDCl_3$): δ = 7.65 (d, J = 9.6 Hz, 1H), 7.28 (d, J = 9.1 Hz, 1H), 7.13 (dd, J_1 = 3.0 Hz, J_2 = 9.1 Hz, 1H), 6.95 (d, J = 3.0 Hz, 1H), 6.44 (d, J = 9.6 Hz, 1H), 4.32 (t, J = 6.1 Hz, 2H), 3.66 ppm (t, J = 6.1 Hz, 2H).

6-{2-[(2-Hydroxyethyl)(methyl)amino]ethoxy}-2*H*-chromen-2-one (1n): A solution of **1m** (0.457 g, 1.70 mmol) in anhydrous THF (15 mL) was cooled to 0 °C, and then DIPEA (1.78 mL, 10.2 mmol) was added followed by 2-(methylamino)ethanol (0.410 mL, 5.10 mmol). The reaction was warmed to room temperature and then held at reflux for 15 h. The solvent was removed under reduced pressure, and the crude oil was purified by flash chromatography (gradient eluent: CH_3OH in EtOAc 0→10%) to yield coumarin intermediate **1n** as a colorless oil (0.412 g, 92%): ^{1}H NMR (300 MHz, [D$_6$]DMSO): δ = 7.98 (d, J = 9.4 Hz, 1H), 7.32 (d, J = 9.1 Hz, 1H), 7.28 (d, J = 2.8 Hz, 1H), 7.18 (dd, J_1 = 3.0 Hz, J_2 = 9.1 Hz, 1H), 6.47 (d, J = 9.6 Hz, 1H), 4.36 (t, J = 5.2 Hz, 1H, dis. with D$_2$O), 4.06 (t, J = 5.8 Hz, 2H), 3.43–3.49 (m, 2H), 2.75 (t, J = 5.8 Hz, 2H), 2.48 (t, J = 6.3 Hz, 2H), 2.26 ppm (s, 3H).

6-{2-[(2-{3-(Dimethylamino)-5-[(triisopropylsilyl)oxy]phenoxy}ethyl)(methyl)amino]ethoxy}-2*H*-chromen-2-one (1o): Intermediate alcohol **1n** (0.263 g, 1.0 mmol) was dissolved in anhydrous THF (3 mL), and then phenol **1e** (0.371 g, 1.20 mmol) was added followed by PPh_3 (0.315 g, 1.20 mmol). The solution was then cooled to 0 °C through an external ice bath, and a solution of DIAD (0.236 mL, 1.20 mmol) in anhydrous THF (2 mL) was added dropwise. The reaction was slowly warmed to room temperature and stirred for 18 h. The solvent was removed under reduced pressure, and the resulting crude mixture was purified by flash chromatography (gradient eluent: EtOAc in *n*-hexane 0→80%) to yield compound **1o** as a dark-brown oil (0.372 g, 67%): ^{1}H NMR (300 MHz, [D$_6$]acetone): δ = 7.90 (d, J = 9.4 Hz, 1H), 7.19–7.24 (m, 3H), 6.39 (d, J = 9.6 Hz, 1H), 5.80–5.85 (m, 3H), 4.17 (t, J = 6.1 Hz, 2H), 4.03 (t, J = 5.8 Hz, 2H), 2.86–2.94 (m, 4H), 2.83 (s, 6H), 2.43 (s, 3H), 1.15–1.32 (m, 3H), 1.11 ppm (d, J = 6.6 Hz, 18H).

6-{2-[{2-[3-(Dimethylamino)-5-hydroxyphenoxy]ethyl}-(methyl)amino]ethoxy}-2*H*-chromen-2-one (20): Intermediate **1o** (0.222 g, 0.40 mmol) was dissolved in anhydrous THF (2.8 mL), and a 1.0 N solution of TBAF (1.20 mL, 1.20 mmol) in THF was slowly added. The mixture was stirred for 30 min at room temperature and then quenched by the addition of saturated aqueous NH_4Cl (5 mL) under stirring for 30 min. After dilution with H_2O (40 mL), the mixture was extracted with Et_2O (3×60 mL). The organic layers were collected, dried over Na_2SO_4, and the solution was concentrated to dryness. The final product was then isolated by flash chromatography (gradient eluent: CH_3OH in EtOAc 0→10%) to obtain a colorless oil (0.145 g, 91%): ^{1}H NMR (300 MHz, [D$_6$]acetone): δ = 7.90 (d, J = 9.4 Hz, 1H), 7.19–7.24 (m, 3H), 6.39 (d, J = 9.6 Hz, 1H), 5.80–5.85 (m, 3H), 4.17 (t, J = 6.1 Hz, 2H), 4.03 (t, J = 5.8 Hz, 2H), 2.86–2.94 (m, 4H), 2.83 (s, 6H), 2.43 ppm (s, 3H), 1 OH not detected; ESIMS m/z: 399 [M+Na]$^+$.

General procedure F for the preparation of ammonium salts 2T–20T, 9D, and 17D: The appropriate amine **2**–**20** (0.070 mmol) was dissolved in anhydrous CH_3CN, and CH_3I (0.044 mL, 0.70 mmol) or CH_3CH_2I (0.056 mL, 0.70 mmol) was added. After stirring for 24 h (for reaction with CH_3I) or 72 h (for reactions with CH_3CH_2I) at room temperature, the starting material disappeared (TLC monitoring). The solvent and excess CH_3I or CH_3CH_2I were then removed under vacuum, and the resulting crude was treated with Et_2O and filtered to give the desired salts.

3-Hydroxy-*N*,*N*,*N*-trimethyl-5-{4-[(2-oxo-2*H*-chromen-7-yl)oxy]butoxy}benzenaminium iodide (2T): Prepared by following general procedure F, starting from amine **2** (0.026 g, 0.070 mmol). Treatment with Et_2O yielded a white solid (0.032 g, 89%): ^{1}H NMR (300 MHz, [D$_6$]acetone): δ = 9.56 (s, 1H, dis. with D$_2$O), 7.91 (d, J = 9.6 Hz, 1H), 7.59 (d, J = 8.5 Hz, 1H), 7.24–7.25 (m, 1H), 7.04 (s, 1H), 6.94 (dd, J_1 = 2.5 Hz, J_2 = 8.5 Hz, 1H), 6.89 (d, J = 2.5 Hz, 1H), 6.71–6.73 (m, 1H), 6.22 (d, J = 9.6 Hz, 1H), 4.23 (t, J = 6.1 Hz, 2H), 4.18 (t, J = 6.1 Hz, 2H), 3.82 (s, 9H), 2.00–2.06 ppm (m, 4H); ESIMS m/z: 384 [M]$^+$.

3-Hydroxy-*N*,*N*,*N*-trimethyl-5-{4-[(3-methyl-2-oxo-2*H*-chromen-7-yl)oxy]butoxy}benzenaminium iodide (3T): Prepared by following general procedure F, starting from amine **3** (0.027 g, 0.070 mmol). Treatment with Et_2O yielded a white solid (0.035 g, 96%): ^{1}H NMR (300 MHz, [D$_6$]acetone): δ = 9.48 (s, 1H, dis. with D$_2$O), 7.70 (s, 1H), 7.50 (d, J = 8.5 Hz, 1H), 7.23–7.24 (m, 1H), 7.02–7.06 (m, 1H), 6.92 (dd, J_1 = 2.5 Hz, J_2 = 8.5 Hz, 1H), 6.87 (d, J = 2.5 Hz, 1H), 6.73–6.74 (m, 1H), 4.07–4.23 (m, 4H), 3.83 (s, 9H), 2.09 (s, 3H), 1.99–2.03 ppm (m, 4H); ESIMS m/z: 398 [M]$^+$.

3-Hydroxy-*N*,*N*,*N*-trimethyl-5-{4-[(4-methyl-2-oxo-2*H*-chromen-7-yl)oxy]butoxy}benzenaminium (4T): Prepared by following general procedure F, starting from amine **4** (0.027 g, 0.070 mmol). Treatment with Et_2O yielded a white solid (0.033 g, 90%): ^{1}H NMR (300 MHz, [D$_6$]acetone): δ = 9.78 (s, 1H, dis. with D$_2$O), 7.69 (d, J = 8.8 Hz, 1H), 7.26–7.27 (m, 1H), 6.99–7.02 (m, 1H), 6.96 (dd, J_1 = 2.5 Hz, J_2 = 8.8 Hz, 1H), 6.88 (d, J = 2.5 Hz, 1H), 6.66–6.67 (m, 1H), 6.13 (s, 1H), 4.17–4.23 (m, 4H), 3.80 (s, 9H), 2.44 (s, 3H), 2.00–2.03 ppm (m, 4H); ESIMS m/z: 398 [M]$^+$.

3-Hydroxy-*N*,*N*,*N*-trimethyl-5-(4-{[2-oxo-4-(trifluoromethyl)-2*H*-chromen-7-yl]oxy}butoxy)benzenaminium iodide (5T): Prepared by following general procedure F, starting from amine **5** (0.031 g, 0.070 mmol). Treatment with Et_2O yielded a red solid (0.036 g, 88%): ^{1}H NMR (300 MHz, [D$_6$]acetone): δ = 7.67–7.70 (m, 1H), 7.32 (t, J = 2.2 Hz, 1H), 7.08 (dd, J_1 = 2.5 Hz, J_2 = 8.8 Hz, 1H), 7.04 (d, J = 2.5 Hz, 1H), 6.97 (t, J = 2.2 Hz, 1H), 6.72 (s, 1H), 6.66 (t, J = 2.2 Hz,

1H), 4.29 (t, $J=5.8$ Hz, 2H), 4.17 (t, $J=5.8$ Hz, 2H), 3.79 (s, 9H), 1.96–2.01 ppm (m, 4H), 1 OH not detected; ESIMS *m/z*: 452 $[M]^+$.

3-{4-[(3-Chloro-4-methyl-2-oxo-2*H*-chromen-7-yl)oxy]butoxy}-5-hydroxy-*N*,*N*,*N*-trimethylbenzenaminium iodide (7T): Prepared by following general procedure F, starting from amine **7** (0.029 g, 0.070 mmol). Treatment with Et_2O yielded a white solid (0.036 g, 93%): ^{1}H NMR (300 MHz, [D$_6$]acetone): $\delta=7.77$ (d, $J=8.8$ Hz, 1H), 7.38–7.39 (m, 1H), 7.02 (dd, $J_1=2.5$ Hz, $J_2=8.8$ Hz, 1H), 6.93–6.95 (m, 2H), 6.64–6.66 (m, 1H), 4.25 (t, $J=5.8$ Hz, 2H), 4.17 (t, $J=5.8$ Hz, 2H), 3.78 (s, 9H), 2.59 (s, 3H), 2.01–2.04 ppm (m, 4H), 1 OH not detected; ESIMS *m/z*: 432 (100) $[M]^+$, 434 (36).

3-({5-[(3-Chloro-4-methyl-2-oxo-2*H*-chromen-7-yl)oxy]pentyl}oxy)-5-hydroxy-*N*,*N*,*N*-trimethylbenzenaminium iodide (8T): Prepared by following general procedure F, starting from amine **8** (0.030 g, 0.070 mmol). Treatment with Et_2O yielded a white solid (0.037 g, 91%): ^{1}H NMR (300 MHz, [D$_6$]acetone): $\delta=9.41$ (s, 1H, dis. with D_2O), 7.77 (d, $J=8.8$ Hz, 1H), 7.15 (t, $J=2.2$ Hz, 1H), 7.05 (t, $J=2.2$ Hz, 1H), 7.01 (dd, $J_1=2.5$ Hz, $J_2=8.8$ Hz, 1H), 6.93 (d, $J=2.5$ Hz, 1H), 6.71 (t, $J=2.2$ Hz, 1H), 4.19 (t, $J=6.3$ Hz, 2H), 4.12 (t, $J=6.3$ Hz, 2H), 3.84 (s, 9H), 2.59 (s, 3H), 1.85–1.98 (m, 4H), 1.66–1.73 ppm (m, 2H); ESIMS *m/z*: 446 (100) $[M]^+$, 448 (34).

3-Hydroxy-*N*,*N*,*N*-trimethyl-5-{4-[(6-oxo-7,8,9,10-tetrahydro-6*H*-benzo[*c*]chromen-3-yl)oxy]butoxy}benzenaminium iodide (9T): Prepared by following general procedure F, starting from amine **9** (0.030 g, 0.070 mmol). Treatment with Et_2O yielded a yellow solid (0.036 g, 92%): ^{1}H NMR (300 MHz, [D$_6$]acetone): $\delta=7.62$ (d, $J=8.8$ Hz, 1H), 7.18 (t, $J=1.9$ Hz, 1H), 7.05 (t, $J=1.9$ Hz, 1H), 6.93 (dd, $J_1=2.5$ Hz, $J_2=8.8$ Hz, 1H), 6.85 (d, $J=2.5$ Hz, 1H), 6.71 (t, $J=1.9$ Hz, 1H), 4.18–4.21 (m, 4H), 3.84 (s, 9H), 2.46–2.48 (m, 4H), 2.01–2.03 (m, 4H), 1.77–1.85 ppm (m, 4H), 1 OH not detected; ESIMS *m/z*: ESIMS *m/z*: 438 $[M]^+$.

***N*-Ethyl-3-hydroxy-*N*,*N*-dimethyl-5-{4-[(6-oxo-7,8,9,10-tetrahydro-6*H*-benzo[*c*]chromen-3-yl)oxy]butoxy}benzenaminium iodide (9D):** Prepared by following general procedure F, starting from amine **9** (0.030 g, 0.070 mmol). Treatment with Et_2O yielded a white solid (0.026 g, 65%): ^{1}H NMR (300 MHz, [D$_6$]acetone): $\delta=7.62$ (d, $J=8.8$ Hz, 1H), 7.06–7.09 (m, 1H), 7.01–7.03 (m, 1H), 6.93 (dd, $J_1=2.5$ Hz, $J_2=8.8$ Hz, 1H), 6.85 (d, $J=2.5$ Hz, 1H), 6.74–6.80 (m, 1H), 4.17–4.23 (m, 4H), 4.16 (q, $J=7.2$ Hz, 2H), 3.78 (s, 6H), 2.79–2.81 (m, 2H), 2.44–2.48 (m, 2H), 1.99–2.04 (m, 4H), 1.74–1.89 (m, 4H), 1.23 ppm (t, $J=7.2$ Hz, 3H), 1 OH not detected; ESIMS *m/z*: 452 $[M]^+$.

3-Hydroxy-*N*,*N*,*N*-trimethyl-5-{4-[(6-oxo-6*H*-benzo[*c*]chromen-3-yl)oxy]butoxy}benzenaminium iodide (10T): Prepared by following general procedure F, starting from amine **10** (0.029 g, 0.070 mmol). Treatment with Et_2O yielded a yellow solid (0.037 g, 95%): ^{1}H NMR (300 MHz, [D$_6$]acetone): $\delta=8.20$–8.30 (m, 3H), 7.88–7.93 (m, 1H), 7.58–7.63 (m, 1H), 7.37–7.39 (m, 1H), 7.11–7.18 (m, 1H), 7.02 (dd, $J_1=2.5$ Hz, $J_2=8.8$ Hz, 1H), 6.94–6.95 (m, 1H), 6.66–6.67 (m, 1H), 4.19–4.41 (m, 4H), 3.78 (s, 9H), 1.98–2.01 ppm (m, 4H), 1 OH not detected; ESIMS *m/z*: 434 $[M]^+$.

3-[(3-{[(3-Chloro-4-methyl-2-oxo-2*H*-chromen-7-yl)oxy]methyl}benzyl)oxy]-5-hydroxy-*N*,*N*,*N*-trimethylbenzenaminium iodide (11T): Prepared by following general procedure F, starting from amine **11** (0.033 g, 0.070 mmol). Treatment with Et_2O yielded a white solid (0.038 g, 90%): ^{1}H NMR (300 MHz, [D$_6$]acetone): $\delta=7.79$ (d, $J=8.8$ Hz, 1H), 7.67 (s, 1H), 7.47–7.51 (m, 3H), 7.38–7.40 (m, 1H), 7.10 (dd, $J_1=2.5$ Hz, $J_2=8.8$ Hz, 1H), 7.01–7.04 (m, 2H), 6.75–6.76 (m, 1H), 5.33 (s, 2H), 5.21 (s, 2H), 3.78 (s, 9H), 2.59 ppm (s, 3H), 1 OH not detected; ESIMS *m/z*: 480 (100) $[M]^+$, 482 (37).

3-Hydroxy-*N*,*N*,*N*-trimethyl-5-{4-[(2-oxo-2*H*-chromen-3-yl)oxy]butoxy}benzenaminium iodide (12T): Prepared by following general procedure F, starting from amine **12** (0.026 g, 0.070 mmol). Treatment with Et_2O yielded a white solid (0.031 g, 87%): ^{1}H NMR (300 MHz, [D$_6$]acetone): $\delta=9.90$ (s, 1H, dis. with D_2O), 7.57–7.60 (m, 1H), 7.41–7.47 (m, 1H), 7.28–7.32 (m, 4H), 6.96–6.99 (m, 1H), 6.67–6.68 (m, 1H), 4.19–4.20 (m, 4H), 3.79 (s, 9H), 2.00–2.03 ppm (m, 4H); ESIMS *m/z*: 384 $[M]^+$.

3-{4-[(6,7-Dimethoxy-2-oxo-2*H*-chromen-3-yl)oxy]butoxy}-5-hydroxy-*N*,*N*,*N*-trimethylbenzenaminium iodide (13T): Prepared by following general procedure F, starting from amine **13** (0.030 g, 0.070 mmol). Treatment with Et_2O yielded a white solid (0.037 g, 92%): ^{1}H NMR (300 MHz, [D$_6$]acetone): $\delta=7.31$ (t, $J=2.5$ Hz, 1H), 7.25 (s, 1H), 7.13 (s, 1H), 6.96 (t, $J=2.5$ Hz, 1H), 6.92 (s, 1H), 6.69 (t, $J=2.5$ Hz, 1H), 4.12–4.20 (m, 4H), 3.89 (s, 3H), 3.84 (s, 3H), 3.79 (s, 9H), 1.99–2.01 ppm (m, 4H), 1 OH not detected; ESIMS *m/z*: 444 $[M]^+$.

3-Hydroxy-*N*,*N*,*N*-trimethyl-5-{4-[(2-oxo-2*H*-chromen-4-yl)oxy]butoxy}benzenaminium iodide (14T): Prepared by following general procedure F, starting from amine **14** (0.026 g, 0.070 mmol). Treatment with Et_2O yielded a yellow solid (0.033 g, 91%): ^{1}H NMR (300 MHz, [D$_6$]acetone): $\delta=7.85$–7.88 (m, 1H), 7.62–7.67 (m, 1H), 7.28–7.37 (m, 2H), 7.11–7.14 (br m, 1H), 7.00–7.02 (m, 1H), 6.70–6.72 (m, 1H), 5.78 (s, 1H), 4.39 (t, $J=6.1$ Hz, 2H), 4.22 (t, $J=6.1$ Hz, 2H), 3.80 (s, 9H), 2.09–2.17 ppm (m, 4H), 1 OH not detected; ESIMS *m/z*: 384 $[M]^+$.

3-Hydroxy-*N*,*N*,*N*-trimethyl-5-{4-[(2-oxo-2*H*-chromen-5-yl)oxy]butoxy}benzenaminium iodide (15T): Prepared by following general procedure F, starting from amine **15** (0.026 g, 0.070 mmol). Treatment with Et_2O yielded a white solid (0.034 g, 95%): ^{1}H NMR (300 MHz, [D$_6$]acetone): $\delta=9.41$ (s, 1H, dis. with D_2O), 8.18 (d, $J=9.9$ Hz, 1H), 7.54 (t, $J=8.5$ Hz, 1H), 7.22 (t, $J=2.2$ Hz, 1H), 7.08 (t, $J=2.2$ Hz, 1H), 6.95 (d, $J=8.5$ Hz, 1H), 6.89 (d, $J=8.5$ Hz, 1H), 6.79 (t, $J=2.2$ Hz, 1H), 6.32 (d, $J=9.9$ Hz, 1H), 4.26–4.30 (m, 2H), 4.19–4.23 (m, 2H), 3.84 (s, 9H), 2.01–2.04 ppm (m, 4H); ESIMS *m/z*: 384 $[M]^+$.

3-Hydroxy-*N*,*N*,*N*-trimethyl-5-{4-[(2-oxo-2*H*-chromen-8-yl)oxy]butoxy}benzenaminium iodide (16T): Prepared by following general procedure F, starting from amine **16** (0.026 g, 0.070 mmol). Treatment with Et_2O yielded a off-white solid (0.033 g, 93%): ^{1}H NMR (300 MHz, [D$_6$]acetone): $\delta=9.41$ (s, 1H, dis. with D_2O), 7.99 (d, $J=9.6$ Hz, 1H), 7.21–7.34 (m, 2H), 7.16–7.20 (m, 1H), 7.12–7.14 (br m, 1H), 7.03–7.05 (m, 1H), 6.71–6.72 (m, 1H), 6.45 (d, $J=9.6$ Hz, 1H), 4.22–4.28 (m, 4H), 3.83 (s, 9H), 1.96–2.02 ppm (m, 4H); ESIMS *m/z*: 384 $[M]^+$.

3-Hydroxy-*N*,*N*,*N*-trimethyl-5-{4-[(2-oxo-2*H*-chromen-6-yl)oxy]butoxy}benzenaminium iodide (17T): Prepared by following general procedure F, starting from amine **17** (0.026 g, 0.070 mmol). Treatment with Et_2O yielded a white solid (0.034 g, 84%): ^{1}H NMR (300 MHz, CD_3OD): $\delta=7.91$ (d, $J=9.6$ Hz, 1H), 7.27–7.30 (m, 1H), 7.15–7.20 (m, 2H), 6.84–6.85 (m, 1H), 6.78–6.79 (m, 1H), 6.52–6.53 (m, 1H), 6.43 (d, $J=9.6$ Hz, 1H), 4.10–4.12 (m, 4H), 3.58 (s, 9H), 1.98–2.02 ppm (m, 4H); ESIMS *m/z*: 384 $[M]^+$.

***N*-Ethyl-3-hydroxy-*N*,*N*-dimethyl-5-{4-[(2-oxo-2*H*-chromen-6-yl)oxy]butoxy}benzenaminium iodide (17D):** Prepared by following general procedure F, starting from amine **17** (0.026 g, 0.070 mmol). Treatment with Et_2O yielded a off-white solid (0.034 g, 92%): ^{1}H NMR (300 MHz, CD_3OD): $\delta=7.91$ (d, $J=9.6$ Hz, 1H), 7.27–7.30 (m, 1H), 7.15–7.20 (m, 2H), 6.75–6.76 (m, 1H), 6.67–6.70 (m, 1H), 6.52–6.54 (m, 1H), 6.43 (d, $J=9.6$ Hz, 1H), 4.09–4.88

(m, 4H), 3.87 (q, $J=7.2$ Hz, 2H), 3.52 (s, 6H), 1.98–2.01 (m, 4H), 1.13 ppm (t, $J=7.2$ Hz, 3H); ESIMS *m/z*: 398 $[M]^+$.

3-Hydroxy-*N*,*N*,*N*-trimethyl-5-({(2*E*)-4-[(2-oxo-2*H*-chromen-6-yl)-oxy]but-2-en-1-yl}oxy)benzenaminium iodide (18T): Prepared by following general procedure F, starting from amine **18** (0.026 g, 0.070 mmol). Treatment with Et_2O yielded a white solid (0.031 g, 87%): ^{1}H NMR (300 MHz, [D$_6$]acetone): $\delta=7.94$ (d, $J=9.6$ Hz, 1H), 7.30–7.34 (m, 1H), 7.21–7.29 (m, 3H), 6.94–6.97 (m, 1H), 6.68–6.69 (m, 1H), 6.42 (d, $J=9.6$ Hz, 1H), 6.14–6.16 (m, 2H), 4.70–4.73 (m, 4H), 3.78 ppm (s, 9H), 1 OH not detected; ESIMS *m/z*: 382 $[M]^+$.

3-Hydroxy-*N*,*N*,*N*-trimethyl-5-({5-[(2-oxo-2*H*-chromen-6-yl)oxy]-pentyl}oxy)benzenaminium iodide (19T): Prepared by following general procedure F, starting from amine **19** (0.027 g, 0.070 mmol). Treatment with Et_2O yielded a yellow solid (0.035 g, 95%): ^{1}H NMR (300 MHz, [D$_6$]acetone): $\delta=7.95$ (d, $J=9.6$ Hz, 1H), 7.25–7.28 (m, 2H), 7.22 (dd, $J_1=2.8$ Hz, $J_2=8.8$ Hz, 1H), 7.06–7.14 (br s, 1H), 6.99 (t, $J=2.2$ Hz, 1H), 6.70 (t, $J=2.2$ Hz, 1H), 6.40 (d, $J=9.6$ Hz, 1H), 4.08–4.12 (m, 4H), 3.81 (s, 9H), 1.83–1.98 (m, 4H), 1.63–1.73 ppm (m, 2H), 1 OH not detected; ESIMS *m/z*: 398 $[M]^+$.

3-[2-(Dimethyl{2-[(2-oxo-2*H*-chromen-6-yl)oxy]ethyl}ammonio)-ethoxy]-5-hydroxy-*N*,*N*,*N*-trimethylbenzenaminium diiodide (20T): Prepared by following general procedure F, starting from amine **20** (0.028 g, 0.070 mmol). Treatment with Et_2O yielded a white solid (0.030 g, 63%): ^{1}H NMR (300 MHz, CD_3OD): $\delta=7.94$ (d, $J=9.6$ Hz, 1H), 6.68–7.20 (m, 6H), 6.43 (d, $J=9.6$ Hz, 1H), 4.21–4.25 (m, 4H), 3.76 (s, 4H), 3.59 (s, 9H), 3.22 ppm (s, 6H).

Biological assays

The inhibition assays of AChE, either from bovine erythrocytes (0.36 U mg^{-1}) or human recombinant (2770 U mg^{-1}), and BChE, from equine serum (13 U mg^{-1}), were run in phosphate buffer (0.1 M, pH 8.0). Acetyl- and butyrylthiocholine iodides were used as substrates and 5,5′-dithiobis(2-nitrobenzoic acid) (DTNB) was used as the chromophoric reagent.[35] Inhibition assays were carried out on an Agilent 8453E UV/Vis spectrophotometer equipped with a cell changer. Solutions of tested compounds were prepared by starting from 10 mM stock solutions in DMSO, which were diluted with aqueous assay medium to a final content of organic solvent always <1%. AChE inhibitory activity was determined in a reaction mixture containing 200 μL of a solution of AChE (0.415 U mL^{-1} in 0.1 M phosphate buffer, pH 8.0), 100 μL of a 3.3 mM solution of DTNB in 0.1 M phosphate buffer (pH 7.0) containing 6 mM $NaHCO_3$, 100 μL of a solution of the inhibitor (six to seven concentrations ranging from 1×10^{-12} to 1×10^{-4} M), and 500 μL of phosphate buffer, pH 8.0. After incubation for 20 min at 25 °C, acetylthiocholine iodide (100 μL of 5 mM aqueous solution) was added as the substrate, and AChE-catalyzed hydrolysis was followed by measuring the increase in absorbance at λ 412 nm for 3.0 min at 25 °C. The concentration of compound that effected 50% inhibition of AChE activity (IC_{50}) was calculated by nonlinear regression of the response–log(concentration) curve, using GraphPad Prism® v. 5. BChE inhibitory activity was assessed similarly using butyrylthiocholine iodide as the substrate. Kinetic studies were performed under the same incubation conditions, using six concentrations of substrate (from 0.033 to 0.2 mM) and four concentrations of inhibitor (0 to 0.9 nM for compound **13** and 0 to 5 nM for donepezil). Apparent inhibition constants and kinetic parameters were calculated within the "enzyme kinetics" module of Prism.

Computational methods

Docking simulations

GOLD (v. 4.1.2), a genetic-algorithm-based software, was used for the docking study, and GoldScore was chosen as a fitness function. Parameters used in the fitness function (hydrogen bond energies, atomic radii and polarizabilities, torsion potentials, hydrogen bond directionalities, etc.) were taken from the GOLD parameter file. In the present study, the 3D coordinates of hAChE (PDB ID: 1B41) and hBChE (PDB ID: 1P0I) were retrieved from the RCSB Protein Data Bank. Rather than the more frequently used *Torpedo californica* form (TcAChE), hAChE was chosen because it has almost identical amino acid residues at both the catalytic and peripheral binding sites, apart from the substitution of Tyr337 (hAChE) with Pro330 (TcAChE).[46] This single residue change was not observed when analyzing primary sequences of either human (PDB ID: 1B41) or bovine (NCBI entry: AA123899.1) AChEs.

The reliability of the docking procedure was validated by the accurate reproduction of the binding conformation of the well-known AChE inhibitor donepezil, whose Cartesian coordinates were extracted from its complex with the TcAChE (PDB ID: 1EVE).[47] Given that the role of water molecules in the AChE binding site is not completely understood, docking simulations were performed without taking water molecules into account.[48]

The target proteins were prepared by adding hydrogen atoms, completing and optimizing missing residues, removing water and the co-crystallized molecules. The basic amino groups were protonated, aromatic amino functional groups were left uncharged, and carboxylic groups were considered to be deprotonated. Molecular docking resulted in 10 poses per inhibitor in a sphere of 10 Å radius centered on the centroid atom of donepezil co-crystallized with TcAChE (PDB ID: 1EVE) previously aligned to hAChE.

Molecular dynamics

Top-scored solutions from molecular docking of compounds **12** and **13** were used as starting points for MD simulations. Complexes of AChE–**12** and AChE–**13** were immersed in cubic TIP3P water boxes that extended 18 Å from the protein atoms and were neutralized by the addition of Na^+ counterions using the AMBER Leap module. This led to simulation systems of 114008 and 114013 atoms for the AChE–**12** and AChE–**13** complexes, respectively. The parm03 version of the all-atom AMBER force field was used to model the system. The solvent molecules were initially relaxed by means of energy minimizations and 30 ps of MD. Subsequently, the full system was minimized to remove bad contacts in the initial geometry and heated gradually to 310 K over 600 ps of MD. The SHAKE algorithm was employed to constrain all R–H bonds, and periodic boundary conditions were applied to simulate a continuous system. A nonbonded cutoff of 12 Å was used, whereas the particle mesh Ewald (PME) method was employed to include the contributions of long-range interactions. The pressure (1 atm) and temperature (310 K) of the system were controlled during the MD simulations by the Langevin method. A 5 ns trajectory was computed for each model with a time-step of 1.5 fs. Coordinates were collected every 2 ps and saved for analysis.

Acknowledgements

The authors are grateful to MIUR, Rome (Italy) for financial support (PRIN, 2008).

Keywords: acetylcholinesterase · Alzheimer's disease · coumarin derivatives · glaucoma · inhibitors

[1] a) M. H. Mohajeri, G. Leuba, *Brain Res. Bull.* **2009**, *80*, 315 – 325; b) R. Cacabelos, *Expert Rev. Mol. Diagn.* **2009**, *9*, 567 – 611; c) D. W. Shineman, H. M. Fillit, *Dialogues Clin. Neurosci.* **2009**, *11*, 129 – 134.

[2] a) H. W. Querfurth, F. M. La Ferla, *New Engl. J. Med.* **2010**, *362*, 329 – 344; b) C. Qiu, M. Kivipelto, E. von Strauss, *Dialogues Clin. Neurosci.* **2009**, *11*, 111 – 128.

[3] F. A. Luque, S. L. Jaffe, *Int. Rev. Neurobiol.* **2009**, *84*, 151 – 165.

[4] F. Noorbakhsh, C. M. Overall, C. Power, *Trends Neurosci.* **2009**, *32*, 88 – 100.

[5] a) M. Citron, *Nat. Rev. Drug. Discovery* **2010**, *9*, 387 – 398; b) R. J. van Marum, *Fundam. Clin. Pharmacol.* **2008**, *22*, 265 – 274; c) G. Pepeu, M. G. Giovannini, *Curr. Alzheimer Res.* **2009**, *6*, 86 – 96; d) J. Rodda, S. Morgan, Z. Walker, *Int. Immunol. Int. Psychogeriatr.* **2009**, *21*, 813 – 824.

[6] H. Kavirajan, *Expert Opin. Drug Saf.* **2009**, *8*, 89 – 109.

[7] a) C. A. Lemere, *Prog. Brain Res.* **2009**, *175*, 83 – 93; b) T. Town, *CNS Neurol. Disord. Drug Targets* **2009**, *8*, 114 – 127.

[8] K. Sugaya, S. Merchant, *J. Alzheimer's Dis.* **2008**, *15*, 241 – 254.

[9] M. Sapra, K. Y. Kim, *Recent Pat. CNS Drug Discovery* **2009**, *4*, 143 – 148.

[10] J. Fan, J. Donkin, C. Wellington, *Biofactors* **2009**, *35*, 239 – 248.

[11] H. C. Huang, Z. F. Jiang, *J. Alzheimer's Dis.* **2009**, *16*, 15 – 27.

[12] M. N. Sabbagh, *Am. J. Geriatr. Pharmacother.* **2009**, *7*, 167 – 185.

[13] a) L. M. Jarvis, *Chem. Eng. News* **2010**, *88*, 12 – 17; b) L. M. Jarvis, *Chem. Eng. News* **2010**, *88*, web exclusive.

[14] N. D. Prins, P. J. Visser, P. Scheltens, *Alzheimer's Res. Ther.* **2010**, *2*, 5.

[15] a) M. Rosini, V. Andrisano, M. Bartolini, M. L. Bolognesi, P. Hrelia, A. Minarini, A. Tarozzi, C. Melchiorre, *J. Med. Chem.* **2005**, *48*, 360 – 363; b) M. Rosini, E. Simoni, M. Bartolini, A. Cavalli, L. Ceccarini, N. Pascu, D. W. McClymont, A. Tarozzi, M. L. Bolognesi, A. Minarini, V. Tumiatti, V. Andrisano, I. R. Mellor, C. Melchiorre, *J. Med. Chem.* **2008**, *51*, 4381 – 4384; c) M. L. Bolognesi, M. Rosini, V. Andrisano, M. Bartolini, A. Minarini, V. Tumiatti, C. Melchiorre, *Curr. Pharm. Des.* **2009**, *15*, 601 – 613.

[16] a) H. Fu, J. Dou, W. Li, W. Cui, S. Mak, Q. Hu, J. Luo, C. S. Lam, Y. Pang, M. B. Youdim, Y. Han, *Eur. J. Pharmacol.* **2009**, *623*, 14 – 21; b) H. Zheng, M. B. Youdim, M. Fridkin, *J. Med. Chem.* **2009**, *52*, 4095 – 4098; c) L. Piazzi, A. Rampa, A. Bisi, S. Gobbi, F. Belluti, A. Cavalli, M. Bartolini, V. Andrisano, P. Valenti, M. Recanatini, *J. Med. Chem.* **2003**, *46*, 2279 – 2282.

[17] C. Brühlmann, F. Ooms, P. A. Carrupt, B. Testa, M. Catto, F. Leonetti, C. Altomare, A. Carotti, *J. Med. Chem.* **2001**, *44*, 3195 – 3198.

[18] A. Carotti, ACS–EFMC Meeting: *Frontiers in CNS and Oncology Medicinal Chemistry*, Siena (Italy), October 7 – 9, **2007**.

[19] a) P. R. Carlier, Y. F. Han, E. S. H. Chow, C. P. L. Li, H. Wang, T. X. Lieu, H. S. Wong, Y. P. Pang, *Bioorg. Med. Chem.* **1999**, *7*, 351 – 357; b) Y. Pang, P. Quiram, T. Jelacic, F. Hong, S. Brimijoin, *J. Biol. Chem.* **1996**, *271*, 23646 – 23649; c) G. Jin, X. Luo, X. He, H. Jiang, H. Zhang, D. Bai, *Arzneim.-Forsch.* **2003**, *53*, 753 – 757; d) M. K. Hu, L. J. Wu, G. Hsiao, M. H. Yen, *J. Med. Chem.* **2002**, *45*, 2277 – 2282.

[20] a) P. Camps, D. Muñoz-Torrero, *Mini-Rev. Med. Chem.* **2001**, *1*, 163 – 174; b) S. Gemma, E. Gabellieri, P. Huleatt, C. Fattorusso, M. Borriello, B. Catalanotti, S. Butini, M. De Angelis, E. Novellino, V. Nacci, T. Belinskaya, A. Saxena, G. Campiani, *J. Med. Chem.* **2006**, *49*, 3421 – 3425; c) P. W. Elsinghorst, W. Härtig, S. Goldhammer, J. Grosche, M. Gütschow, *Org. Biomol. Chem.* **2009**, *7*, 3940 – 3946.

[21] a) R. Morphy, Z. Rankovic, *Drug Discov. Today* **2007**, *12*, 156 – 160; b) C. A. Manssour Fraga, E. J. Barreiro, *Curr. Drug Ther.* **2008**, *3*, 1 – 13.

[22] M. I. Fernández-Bachiller, C. Pérez, N. E. Campillo, J. A. Páez, G. C. González-Muñoz, P. Usán, E. García-Palomero, M. G. López, M. Villarroya, A. G. García, A. Martínez, M. I. Rodríguez-Franco, *ChemMedChem* **2009**, *4*, 828 – 841.

[23] O. Weinreb, S. Mandel, O. Bar-Am, M. Yogev-Falach, Y. Avramovich-Tirosh, T. Amit, M. B. Youdim, *Neurotherapeutics* **2009**, *6*, 163 – 174.

[24] J. Marco-Contelles, R. León, C. de Los Ríos, A. Samadi, M. Bartolini, V. Andrisano, O. Huertas, X. Barril, F. J. Luque, M. I. Rodríguez-Franco, B. López, M. G. López, A. G. García, M. do Carmo Carreiras, M. Villarroya, *J. Med. Chem.* **2009**, *52*, 2724 – 2732.

[25] J. Zhang, D. Zhu, R. Sheng, H. Wu, Y. Hu, F. Wang, T. Cai, B. Yang, Q. He, *Eur. J. Pharmacol.* **2009**, *613*, 1 – 9.

[26] a) P. Munoz-Ruiz, L. Rubio, E. Garcia-Palomero, I. Dorronsoro, M. del Monte-Millan, R. Valenzuela, P. Usan, C. de Austria, M. Bartolini, V. Andrisano, A. Bidon-Chanal, M. Orozco, F. J. Luque, M. Medina, A. Martinez, *J. Med. Chem.* **2005**, *48*, 7223 – 7233; b) N. C. Inestrosa, J. P. Sagal, M. Colombres, *Subcell. Biochem.* **2005**, *38*, 299 – 317.

[27] N. C. Inestrosa, M. C. Dinamarca, A. Alvarez, *FEBS J.* **2008**, *275*, 625 – 632.

[28] a) M. B. Youdim, J. J. Buccafusco, *J. Neural Transm.* **2005**, *112*, 519 – 537; b) A. Cavalli, M. L. Bolognesi, A. Minarini, M. Rosini, V. Tumiatti, M. Recanatini, C. Melchiorre, *J. Med. Chem.* **2008**, *51*, 347 – 372.

[29] F. Leonetti, M. Catto, O. Nicolotti, L. Pisani, A. Cappa, A. Stefanachi, A. Carotti, *Bioorg. Med. Chem.* **2008**, *16*, 7450 – 7456.

[30] E. Giacobini, *Butyrylcholinesterase: Its Function and Inhibitors*, Thomson Publishing Services, **2003**.

[31] B. V. Rama Sastry in *Burger's Medicinal Chemistry and Drug Discovery, 6th Ed.* (Ed: D. J. Abraham), Wiley, New York, **2003**, pp. 109 – 166.

[32] Y. A. Jackson, *Heterocycles* **1995**, *41*, 1979 – 1986.

[33] T. Harayama, K. Katsuno, N. Nishioka, M. Fujii, Y. Nishita, H. Isii, Y. Kaneko, *Heterocycles* **1994**, *39*, 613 – 622.

[34] T. Petrzilka, W. G. Lusuardi, *Helv. Chim. Acta* **1973**, *56*, 510 – 518.

[35] G. L. Ellman, K. D. Courtney, V. Andres, Jr., R. M. Feather-Stone, *Biochem. Pharmacol.* **1961**, *7*, 88 – 90.

[36] M. L. Verdonk, J. C. Cole, M. J. Hartshorn, C. W. Murray, R. D. Taylor, *Proteins Struct. Funct. Bioinf.* **2003**, *52*, 609 – 623.

[37] D. A. Case, T. A. Darden, T. E. Cheatham III, C. L. Simmerling, J. Wang, R. E. Duke, R. Luo, M. Crowley, R. C. Walker, W. Zhang, K. M. Merz, B. Wang, S. Hayik, A. Roitberg, G. Seabra, I. Kolossváry, K. F. Wong, F. Paesani, J. Vanicek, X. Wu, S. R. Brozell, T. Steinbrecher, H. Gohlke, L. Yang, C. Tan, J. Mongan, V. Hornak, G. Cui, D. H. Mathews, M. G. Seetin, C. Sagui, V. Babin, P. A. Kollman, AMBER 10, **2008**, University of California, San Francisco.

[38] J. C. Phillips, R. Braun, W. Wang, J. Gumbart, E. Tajkhorshid, E. Villa, C. Chipot, R. D. Skeel, L. Kale, K. Schulten, *J. Comput. Chem.* **2005**, *26*, 1781 – 1802.

[39] L. Savini, A. Gaeta, C. Fattorusso, B. Catalanotti, G. Campiani, L. Chiasserini, C. Pellerano, E. Novellino, D. McKissic, A. Saxena, *J. Med. Chem.* **2003**, *46*, 1 – 4.

[40] H. Sugimoto, H. Ogura, Y. Arai, Y. Iimura, Y. Yamanishi, *Jpn. J. Pharmacol.* **2002**, *89*, 7 – 20.

[41] H. M. Berman, J. Westbrook, Z. Feng, G. Gilliland, T. N. Bhat, H. Weissig, I. N. Shindyalov, P. E. Bourne, *Nucleic Acids Res.* **2000**, *28*, 235 – 242.

[42] Y. Cheng, X. Cheng, Z. Radić, J. A. McCammon, *J. Am. Chem. Soc.* **2007**, *129*, 6562 – 6570.

[43] a) H. von Pechmann, C. Duisberg, *Ber. Dtsch. Chem. Ges.* **1883**, *16*, 2119 – 2128; b) S. Sethna, R. Phadke, *Org. React.* **1953**, *7*, 1 – 58.

[44] O. Gia, E. Uriarte, G. Zagotto, F. Baccichetti, C. Antonello, S. Marcianimagno, *J. Photochem. Photobiol. B* **1992**, *14*, 95 – 104.

[45] L. Leonetti, A. Cappa, C. Maccallini, A. Carotti, *Arkivoc* **2004**, *v*, 272 – 285.

[46] X. Barril, M. Orzoco, F. J. Luque, *J. Med. Chem.* **1999**, *42*, 5110 – 5119.

[47] J. L. Sussman, M. Harel, F. Frolow, C. Oefner, A. Goldman, L. Toker, I. Silman, *Science* **1991**, *253*, 872 – 879.

[48] J. Guo, M. M. Hurley, J. B. Wright, G. H. Lushington, *J. Med. Chem.* **2004**, *47*, 5492 – 5500.

Received: May 13, 2010
Revised: June 25, 2010
Published online on August 2, 2010

